University of Mosul
College of Veterinary Medicine

The Impact of Selenium Nanoparticles on the Healing of Induced Radial Bone Fracture in Dogs

Marwan Mahmood Abed Khalaf

MSc. Thesis

Veterinary Medicine / Veterinary Surgery

Supervised By

Assistant Professor

Dr. Omar Adil Bader

2025 A.D. **1446 A.H.**

The Impact of Selenium Nanoparticles on the Healing of Induced Radial Bone Fracture in Dogs

A Thesis Submitted

By

Marwan Mahmood Abed Khalaf

To

The council of the College of Veterinary Medicine

University of Mosul

In

Partial Fulfillment of the Requirements

For the Degree of Master of Science

In

Veterinary Medicine / Veterinary Surgery

Supervised By

Assistant Professor

Dr. Omar Adil Bader

2025 A.D. **1446 A.H.**

بسم الله الرحمن الرحيم


ذَٰلِكَ فَضْلُ اللَّهِ يُؤْتِيهِ

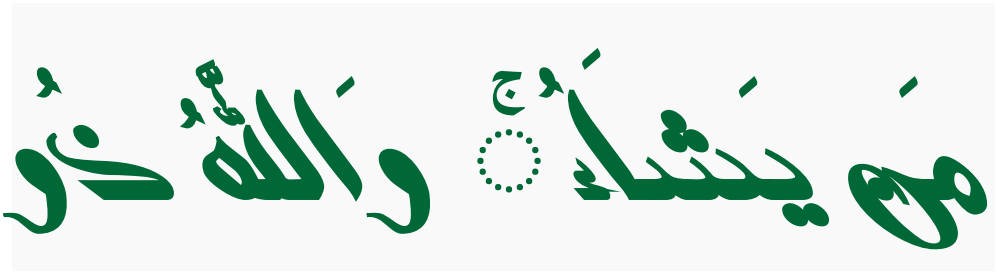
مَن يَشَاءُ ۚ وَاللَّهُ ذُو

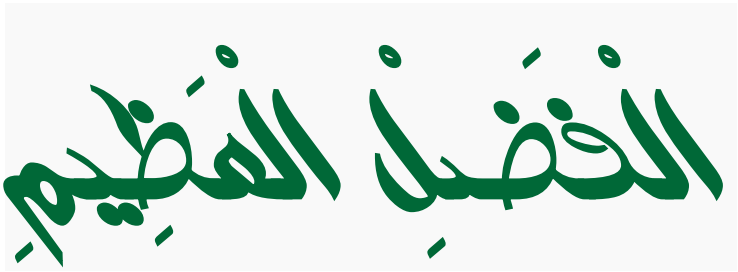
الْفَضْلِ الْعَظِيمِ

الجمعة الآية (٤)

Supervisor Certification

I certify that this thesis entitled "**The Impact of Selenium Nanoparticles on the Healing of Induced Radial Bone Fracture in Dogs**" was prepared under my supervision at the College of Veterinary Medicine / University of Mosul, as a partial fulfillment of the requirements for the degree of MSc. in Veterinary Medicine / Veterinary Surgery.

Signature:
Name: **Assist. Prof Dr. Omar Adil Bader**
Date: 7 / 1 / 2025

Linguist Certification

I certify that this thesis entitled "**The Impact of Selenium Nanoparticles on the Healing of Induced Radial Bone Fracture in Dogs**" has been linguistically reviewed and corrected for language and expression mistakes; therefore, it becomes ready for the defense as for as the integrity of the writing and expression.

Signature:
Name: **Assist. Prof Dr. Qusai Basheer Ibrahim**
Date: 19 / 1 / 2025

Statistic Certification

I certify that this thesis entitled "**The Impact of Selenium Nanoparticles on the Healing of Induced Radial Bone Fracture in Dogs**" has been statistically reviewed and corrected for statistic and expression mistakes; therefore, it becomes ready for the defense as for as the integrity of the statistic and expression.

Signature:
Name: **Lec. Dr. Zaid Triq Saleh**
Date: 18 / 1 / 2025

Department of Surgery and Theriogenology Head Certification

Based on the supervisor, linguistics and statistic recommendations, I forward this thesis for the defense.

Signature:
Name: **Prof. Dr. Mohammed Abdalelah Aziz**
Date: 22 / 1 / 2025

Postgraduate Committee Director Certification

Based on the supervisor, linguistics, statistic and the Head of the Department Surgery and Theriogenology recommendations, I forward this thesis for the defense.

Signature:
Name: **Prof. Dr. Raad Abdulghany Al-Sanjary**
Date: 30 / 1 / 2025

Examination Committee Decision

We, the members of the Evaluation and Discussion Committee, have reviewed this thesis and discussed the student **Marwan Mahmood Abed** in its contents on 25 / 2 / 2025, and certify that he deserves the degree of MSc in Veterinary Medicine / Veterinary Surgery.

Signature
Lecturer
Dr. Firas Mohammed Abed
Member

Signature
Assistant Professor
Dr. Sahar Mohammed Ibrahim
Member

Signature
Assistant Professor
Dr. Omar Adil Bader
Member and Supervisor

Signature
Assistant Professor
Dr. Moyaser Ghanim Thanoon
Chairman

College Council Decision

The College of Veterinary Medicine Council was met, the meeting on / / 2025, and decided to award him a degree of MSc. in Veterinary Surgery.

Signature
Professor
Dr. Raad Abdulghany Al-Sanjary
Assistant Dean for Scientific Affairs

Signature
Professor
Dr. Dhafer Mohammad Aziz
Dean

Acknowledgement

I thank **God Almighty** for his protection in my life and for allowing me to succeed in all periods of my studies.

I express my thanks and gratitude to the **staff of the College of Veterinary Medicine / University of Mosul** for providing me with unlimited support to complete this study.

I am very indebted and grateful to my supervisor, **Assistant Professor Doctor Omar Adil Bader**, for his great help, support, endless advice, patience, and suggestions for presenting this work in the most comprehensive, clear, and accurate way.

Last but not least, I want to express my appreciation to all the academic and technical **staff of the Department of Surgery and Theriogenology** and the **Animal House Center** at the College of Veterinary Medicine / University of Mosul for their tremendous support and patience that have contributed to the success of this work.

Marwan Mahmood Abed

Abstract

The aim of this study was to evaluate the role of selenium nanoparticles (Se-NPs) on the healing of distal radial fracture in dogs. Twenty four clinically healthy adult male dogs have been used in this study, weighing (25 ± 0.5) kg and aged (2 ± 0.5) years. The experimental animals were divided randomly into two equal groups. Under general anesthesia all experimental animal has been submitted to induced transverse fracture at the distal part of radial bone by using wire saw.

In the first group (control group) the transverse fracture was left without adding any material, then was reduced and fixed by fiber glass cast tape and left to heal without adding any material, the Second group (treated group) was treated by pouring the selenium nanoparticles (Se-NPs) on the fracture line, reduction and fixation by fiber glass cast tape was done. The impact of Se-NPs on the fracture healing is evaluated by clinical observation, radiographical examination, histopathological examination and histochemical examination at 2^{nd}, 4^{th}, 6^{th} and 8^{th} week post operation.

The clinical examination of dogs revealed a more rapid return to the normal function in the treated group compared to the control one, as evidenced by earlier resolution of lameness and earlier weight-bearing on the affected limb. The radio-graphical examination has showed better fracture healing in the treated group and faster than in control group by increase periosteal reaction in early stages, then adequate in callus formation and faster remodeling in treated group in contrast to control one. The microscopical examination has shown superiority of treated group by good response to fracture healing, the microscopical examination has shown increase of fibrocartilaginous tissue at early stage,

then increase of osteoblasts at middle stages with decrease of osteoclasts with formation of haversian system with arrangement of osteocytes around the canal of haversian system and at the last stages appeared of formation of compact lamellar bone, mature bone contain osteocytes in their lacunae.

The conclusion of this study is that Se-NPs can accelerate and enhance the healing of distal radial bone fracture.

Contents

List of Abbreviation and Symbols

BMSCs	**Bone marrow mesenchymal stem cells**
Se NPs	Selenium nano particles
BMP-2	Bone morphogenetic protein
ROS	Reactive oxygen species
MSCs	Mesenchymal stem cells
Se	Selenium
Nm	Nanometer
KV	Kilovolt
mA	Milliamperage
IU	International unit
IL	Interleukin
TNF	Tumor necrosis factor
IGF	Insulin-like growth factor
TGF-β	Transforming growth factor-β
PDFG	Platelet-derived growth factor
IFN-γ	Interferon-γ
PK	Pharmacokinetic

PLA	Pulsed laser ablation
FFD	Field focus distance
OS	Oxidative stress
GPx	Glutathione peroxidase
TrxR	Thioredoxin reductase
COX	Cyclooxygenase
µg	Microgram
Mg	Milligram
ALP	Alkaline phosphatase
VEGF	Vascular endothelial growth factor
SeCys 2	Selenocysteine
LNT-Se	Lentinan Se
PTHrP	Parathyroid hormone related protein
NB	Newly bone
OB	Old bone
BV	Blood vessels
CC	Chondrocytes
IC	Intra cartilaginous
IBC	Intra bony callus
TT	Thick trabeculae
FB	Fibroblast
FCT	Fibrous connective tissue
OM	Osteo-matrix
HS	Haversian system

List of Tables

List of Figures

Chapter One

Introduction

Orthopedists are troubled by the critical issue of delayed or failed bone union which is the challenges that face them; in fact, over 70% of patients with catastrophic injuries require at least one orthopedic surgery (Li *et al*., 2019). One of the most common fractures that challenge orthopedists in dogs are the radius and ulna fractures which are considered the third most prevalent fractures (Watrous & Moens, 2017).

Radius is the forelimb bone in dogs that bears the most weight, and according to statistics fractures of the radius make up 43.1% of long bone fractures and 36.5% of total fractures (Popovitch *et al*., 2019). The distal radial fractures are accounted for 85% of radial fractures (Harasen, 2003a). So, in most forearm fractures the distal part of the antebrachium is mostly damaged because its relatively little soft tissue coverage and poor vascularization (Kim & Kim, 2024). The most prevalent fractures causes are car accidents, height falls and fighting between dogs (Libardoni *et al.*, 2016).

Delay or failure of the bone union which is present in the distal radial fractures occurs in small breeds that having decreased density of intraosseous and extraosseous blood supply (Harasen, 2003b). The most common technique used for fracture repair is the external fixation, however such technique has no avail in small breeds because delay union when compared with large breed (McCartney *et al.*, 2010).

Advanced discovery of new materials nano sciences and nanotechnology are driving a global technological revolution (Bindhu *et al*., 2016). Nanomedicine, the specialized use of nanotechnology in the healthcare system, has arisen to offer fresh approaches to the unresolved side effects of medicine (Kargozar and Mozafari, 2018).

In many fields, selenium (Se) has paid a lot of attention. Trace amounts of this element are necessary for life. As an antioxidant, selenium plays a crucial role in the regulation of reactive oxygen species (ROS) and is known to influence several physiological processes, such as cell differentiation and anti-inflammatory properties (Lee *et al*., 2021).

Histopathological techniques are valuable for confirming the examination observations so, histochemistry achieved by special stains such as Masson Trichrome, which is used to differentiate between collagen and muscle fiber, Alizarin red stain for the detection and visualization of mineralized tissues, particularly calcium deposition in bone, and Alcian blue stain is used to detect cartilaginous tissue (Soyab, 2020; Salian, 2021).

Regarding medical use of Nano particles, Selenium enters metabolic pathways within the body to form proteins called Seleno-proteins which are composed of a group of amino acids, these proteins differ in their functions and physiological actions, some of which act as antioxidants, selenium transporters stores protein (Seleno-proteins) in addition to their role in calcium metabolism and thyroid hormone (Sreelatha *et al*., 2018; Kang *et al*., 2020).

Yang *et al* 2022 mentioned that one of the major challenges that there are a limited studies on the therapeutic effects of Se-NPs on pathological conditions associated with bones. This study evaluates the role of Se-NPs as a stimulating and accelerating factor for the healing process of the radius bone in dogs. Selenium can improve immune surveillance, control bone marrow mesenchymal stem cells (BMSC) differentiation and proliferation, and shield BMSCs from oxidative stress-related damage (Zeng *et al*., 2013), also, Se deficit increases bone resorption, which is harmful to bone microarchitecture (Cao *et al*., 2012).

To overcome the problem of delayed or non-healing of radius bone fractures and in order to benefit from the stimulating advantages for bioactive materials in stimulating healing, this study is designed and aims at:

Evaluation of selenium nanoparticles activity on the healing of distal radial fractures by using the following parameters:

1- Clinical evaluation at all periods of study.
2- Radio-graphical evaluation at two, four, six and eight weeks.
3- Histopathological evaluation at two, four, six and eight weeks.

Chapter Two

Literature Review

2.1 Anatomy of bone

Bone (osseous tissue) is the body's hardest tissue, it is a highly vascularized, mineralized connective tissue, most vertebrate’s skeleton is made of bones which provide mechanical support, its stable under tension and compression, and deformation resistance. They maintain their maximum weight and enable effective movement when paired with muscles, tendons, and ligaments (Blumer, 2021).

Generally, a solid cortical bone is the outer layer of bone, while the interior spongy bone structure, is known as cancellous or trabecular bone. Different trabeculae organized in a honeycomb arrangement constitute the trabecular bone. The skeletal segments and their functions determine the relative proportion of cortical and trabecular bone. The major difference between cancellous and compact bone lies in their porosity that ranges from 30% and 90% in the cancellous bone, while between 5% to 30% in the compact bone. Three sections make up the long bones (as the femur and humerus): diaphysis, which is the center shaft; epiphysis, which is the bulbous extremities; and metaphysis, which is situated in between the two. A medullary (marrow cavity), is located in the center of the shaft, it holds in infancy stage the red bone marrow which responsible for hematopoiesis and in adulthood stage hold more yellow marrow which responsible for energy storage (Tozzi *et al*., 2016).

The special stiffness and strength that allow bone to sustain physiological loads without breaking are a result of both the material characteristics of bone and the structure of entire bones, furthermore bone serves as a storehouse for numerous vital minerals, including calcium and phosphate, and it is crucial for controlling the amounts of ions in extracellular fluid and also the “mesenchymal stem cells” (MSCs) which consider pluripotent cells that present in the bone marrow that have ability to differentiate into (bone, cartilage, tendon, muscle, dermis, and also fat) (Mistry and Mikos, 2005).

2.2 Anatomical feature of dog antebrachium region

The ante brachium region is the part of forelimb that extends from elbow joint to carpal joint and consist of radius and ulna bones. The most blood supply of the ante brachium is from median artery, ulnar artery and the radial artery, while the nerve supply is from radial nerve and ulnar nerve in addition to median nerve (Levine *et al*., 2007). The fore limb of dog has possessed accessory structures such as olecranon process and anconeal process (Shapiro, 2008).

There are two groups of muscles in antebrachium region, the extensor and flexor muscles, the extensor group include Extensor carpi radialis, Ulnaris lateralis, Lateral digital extensor muscle, while the flexor muscles include, Flexor carpi radials muscle, Flexor carpi ulnaris muscle, Deep digital flexor muscle and Superficial digital flexors muscle (Evans and Alexander, 2017).

2.3 Radius bone in the dog

Dogs have rather long ulnas and radiuses that articulate with one another at their extremities to create a small interosseous gap that allows for some movement. With a concave surface for articulation with the humerus above and a convex marginal area for the ulna posteriorly, the proximal extremity of the radius is tiny. The ulna's concave facet is located laterally, and the distal extremity is broad with a medial border that extends downward to produce the styloid process of the radius (Belu *et al*., 2021).

2.3.1 Radial bone blood supply

The main source for the radial bone blood supply is the nutrient artery, in addition to its related branches and the metaphyseal arteries in two extremities of the radius, the radius bone possesses only one nutrient foramen in the proximal part and from this foramen the nutrient artery inters the bone then branch out toward the diaphyseal bone's ends within the marrow cavity and extend distal to elbow joint (Sim and Ahn, 2014), and because of the present of nutrient foramina in the proximal part only, this led to make the distal part of the bone poor with blood supply (Della Nina *et al*., 2007; Decamp *et al*., 2016). Also, significant intracortical anastomoses exist between the outer periosteal and inner medullary arteries (Shapiro, 2008).

2.3.2 Nerve supply of radial bone

The brachial plexus extends from the 5^{th} cervical vertebra to the 1^{st} thoracic vertebra and give many branches, one of these branches is the radial nerve which derived from the posterior part of plexus and supply the superior portion of radius bone, then extend to the triceps muscle of

fore arm, anconeus muscle, posterior extensors muscle, and also supply the carpal joint and dorsal part of antebrachium (Latef *et al*., 2018; Gragossian and Varacallo, 2020).

The radial nerve supply combined with the blood supply and divided to three types of nerves such as sensory nerves, sympathetic nerves and parasympathetic nerves which have a role in regulation of the bone cells blood supply in addition to its specific role in perception of pain also play role in growth of bone by network formation in highly metabolic area in the bone (Zhang *et al*., 2016).

2.4 Histology and physiology of bone

The multipotent mesenchymal stem cells can be differentiated into the osteoprogenitor cells throughout embryogenesis. These cells are either the osteoblasts which make the bone, or the chondrocytes that serve as the model for the endochondral ossification. Homeostasis and development of bone depend on several types of cells. The tissue of bone contains, osteocytes, osteoblasts and also the osteoclasts (Hernandez-Gil *et al*., 2006).

The osteoid matrix is joined by non-collagenous proteins which promote calcium and phosphate adhesion, resulting in the mineralization and organization the forming new bone tissue. when mineralization takes place, the osteoblasts transform into osteocytes if they are present within the osteoid matrix (Kini and Nandeesh, 2021).

Central to the osteon main components are osteocytes, which can use canaliculi to transfer mechanical stresses to neighboring osteocytes and cells lining the bone (Dutta and Dutta, 2013; Brannigan and Griffin, 2016). It is believed that this intercellular connection promotes mineral

transport between blood and bone as well as bone resorption and production (Kini and Nandeesh,2012).

The differentiated macrophages stimulated by cytokines are called osteoclasts (Bernstein, 2011), they are found near the surface of the bone (James *et al*., 2011), they resorb mature bone by secreting enzymes that break down proteins and acids (Dutta and Dutta, 2013), the pace at which minerals from this breakdown are transferred from the bone into the bloodstream is controlled by bone lining cells (James *et al*., 2011; Brannigan and Griffin, 2016).

The endochondral formation of bone process, which is shown at the embryogenesis of both types of bone (short and long bones), is the primary pathway for bone creation. As chondrocytes mature, they generate a matrix rich in collagen. When these cells reach maturity, they stop dividing and start to make proteins that cause the matrix to become calcified. Phagocytes are responsible for the cartilaginous matrix's resorption (Brannigan and Griffin, 2016).

2.4.1 Histopathological techniques

Histopathological techniques such as a routine stains as H&E stains to detect nucleus and cytoplasm, histochemical staining by using special stains such as Masson Trichrom which used to detect collagen fiber, Alizarin red stain which is used to detect calcium deposition, Alcian blue stain which is used to detect cartilaginous tissue, while immunohistochemical staining is used to detect specific epitope of target protein of interest, either intracytoplasmic or intra nuclear (Borch *et al*., 2019; Soyab, 2020; Salian, 2021).

2.5 Fractures

Fracture can be defined as a disruption or deformation of the normal architecture and continuity of the bone, fracture can be acute, subacute or chronic. Subacute and chronic fractures, while frequently needing treatment, can often be managed on an ambulatory basis and do not require emergent care. Acute fractures can be differentiated radiographically from older fractures by the identification of sharp, well-defined edges of the fragments. Sever callus development and a blunting edge may be visible in older fractures (Dowson *et al*., 2022).

The fracture may be complete or incomplete and sometimes segmented to many fragments in severe cases. Disruption may be extended to soft tissue in variable degrees such as bruise of muscles and disruption of blood vessels and skin. Fracture can be occurred due to high stress during pressing or wrong movement, also occur due to the pathological conditions as osteoporosis, osteosarcoma and osteogenesis imperfect. The value of radial and ulnar fracture about 17% from the general fractures in dogs, which occur due to fall from the height sites or car accident (Astur *et al*., 2016; Witmer *et al*., 2016).

2.5.1 Classification of fracture

To choose the correct method of fracture treatment, we must know the type of fracture, so fractures can be classified according to the following:

2.5.1.1 According to the skin involvement

a. Closed fracture: in this type of fractures the skin is intact without disruptions.

b. Open fracture: the skin in the fracture site disrupted and affected with open wounds, and the bone sometimes protrude from the wound and contact with external environment (Oryan *et al*., 2013).

2.5.1.2 According fracture causes

a. Traumatic fracture: it occurs due to car accidents, falling injuries and fighting between animals.
b. Pathologic fracture: caused by some pathological affection of the bone tissue such as osteosarcoma, osteoporosis and other systemic diseases such as hormonal disturbance of parathyroid gland (Oryan *et al*., 2013).

2.5.1.3 According to bone displacement

a. Displaced: no alignment of fracture segments at the fracture line.
b. Non-Displaced: alignment of fracture line without displacement (Kellam *et al*., 2018).

2.5.1.4 According to fracture orientation

a. Linear type fracture: the fracture line is parallel to bone axis.
b. Transverse type fracture: the line of fracture is perpendicular to bone longitudinal axis.
c. Oblique type fracture: the line of fracture is obliquely to the axis of bone.
d. Spiral type fracture: the line of fracture is spiral with twisting of the bone.

e. Comminuted fracture: occur due to sever direct force and the fractured bone has more than two fragments (Oryan *et al*., 2013; Ali, 2013).

2.5.1.5 According to bone tissue damage severity

a. Incomplete fracture: it is also called greenstick type fracture occur in cases of the bone cracks and bone bends but does not completely break.
b. Complete fracture: it is breaking the bone to separated pieces (Oryan *et al*., 2013).

2.5.1.6 Anatomical long bone location

A fracture is classified according to its location in the bone body, such as proximal fracture, distal fracture, diaphyseal, metaphyseal, epiphyseal and growth plate fractures (Bennour *et al*., 2014; Kellam *et al*., 2018).

2.5.2 Fracture healing

Fracture healing is a tissue regeneration mechanism in which a series of events take place after bone fracture which result in the restoration and preservation of the bone's mechanical and physical characteristics to restore state that extremely similar to that before bone damage. Modulating these factors and developing innovative methods and therapies to treat nonunion and delayed unions have been made possible by understanding the cells that involved in this process and the role of growth factors, with their interactions with the extracellular matrix scaffold, and the mechanical stability at the site of fracture that influencing on the type of tissue which made up between the fracture bone segments (Shenoy and Pillai, 2017).

In the histological classical terms, fracture healing can be divided into two types including primary fracture healing (direct) and secondary healing (indirect) (Oryan *et al*., 2015).

2.5.2.1 Direct (Primary) type of fracture healing

Primary healing of fracture is considering a faster healing process that occur after using a specific devices of bone fixation (bone plates with screws) which are used for make up the fracture sites approximated firmly. Direct healing occurs when necessitates rigid fixation is present, and it can be occurred only in complete absence of motion under physiological load on both ends of fractured bone. Lamellar bone begins to synthesized by osteoblasts action, beginning parallel to the bone longitudinal axis across the site of fracture, without showing any signs to callus formation. Gap healing and contact healing are two distinct forms of direct healing of bone that rely on the voids between fracture segments. An anatomically accurate and biomechanically competent lamellar bone structure is attempted to be immediately restored in both procedures (Marsell and Einhorn, 2011; Giganti *et al*., 2014; Oryan *et al*., 2015).

2.5.2.2 Indirect (Secondary) type of fracture healing

There are more than one terms for indirect fracture healing such as, secondary healing, endochondral ossification and callus healing. Steps of indirect healing are beginning by impaction respected by inflammation, development primary soft callus, mineralization of callus, and remodeling of callus. It’s usually arising after intramedullary nailing and external fixation techniques, and it is usually happening when there might be any micro-motions occur between the ends of fracture. The motion usually promotes this kind of healing of fracture, while it is inhibited by tight

immobilization, the secondary model of fracture healing involves the intramembranous and endochondral bone healing (Dimitriou *et al*., 2005; Marsell and Einhorn, 2011; Myo *et al*., 2016).

Secondary fracture healing can be divided into (inflammatory phase, proliferative phase and remodeling phase, these stages may be overlapped and had an impact on one another when the fracture healed (Cottrell *et al*., 2016).

2.5.2.2.1 Inflammatory phase

The first step occurs immediately after fracture, which is the hematoma formation in the fractured bone (Mountziaris and Mikos, 2008). Hematoma occurs due to bleeding from injured bone and the periosteal injured vessels that are formed beneath the periosteum and within the medullary canal. The degranulated platelets that present in the hematoma release potent vasoactive mediators by activated coagulation system (Schell *et al*., 2017).

Within the first week following the injury, there is a large increase in a number of inflammatory mediators, including cytokines like interleukin-1 (IL -1), interleukin -6 (IL -6), interleukin- 11 (IL -11), interleukin -8 (IL-18), and tumor necrosis factor -α (TNF-α) (Mountziaris and Mikos, 2008). After that, platelets continue to aggregate and new blood vessels (angiogenesis) begin to form (Dimitriou *et al.,* 2005).

Following to vascular injury the fracture site suffered from hypoxia, so the osteocytes at the margin of the fracture site undergo malnutrition, degeneration and necrotic changes (Geris *et al.*, 2008).

The macrophages release signaling factors to phagocytize the necrotic regions and promote the regeneration stage. There are many types of growth factors such as insulin -like growth factor (IGF), transforming growth factor -β (TGF-β), platelet -derived growth factor (PDGF), and bone morphogenic proteins (BMP -2, BMP -5, BMP -7) are important and necessary for these steps, so the cells migration, recruitment, proliferation, and the differentiation of mesenchymal stem cells into, fibroblasts, chondroblasts, angioblasts and osteoblasts are triggered by these growth factors (Lastayo *et al*., 2003).

The fracture gap filled by participation of, fibroblasts, endothelial cells and osteoblasts that formation the granulation tissue (Goldhahn *et al*., 2012). Osteoblasts have a role in communicating with vascular endothelial cells and thus have an effect not only in the formation of osteogenic matrix but also stimulates the formation of blood vessels (angiogenesis) which work to transport oxygen and nutrients to the renewed bone tissue as osteoblasts secrete factors that stimulate the formation of blood vessels such as vascular endothelial growth factor (VEGF) and erythropoietin, also osteoblasts secrete the factor CXcl 9 that mediates the communication between osteoblast and endothelial cells during bone regeneration and thus the accelerate of angiogenesis leads to accelerating the process of bone healing (Rankin *et al*., 2012; Huang *et al*., 2016).

2.5.2.2.2 Proliferative phase

Essentially, the way by which the fracture hematoma is organized has been used to characterize the proliferative or fibroplasia phase. Necrotic bone resorption occurs during the fibroplasia phase and is mediated by osteoclasts, and this osteoclast are generated from

monocytes in the circulation and the monoblastic precursor cells which arising from bone marrow locally (Sheen *et al*., 2023).

Callus formation, persistent of vascular ingrowth, secretion of osteoid, and the presence of collagen fibers are the hallmarks of the fibroplasia phase (Pilitsis *et al*., 2002). The recent woven bone created by intramembranous or endochondral bone production gradually replaces the periosteal response, which includes angiogenesis, formation of connective tissue and formation of soft callus (Goldhahn *et al*., 2012)

The mesenchymal stem cells can be differentiated into chondroblasts which are the cells responsible for cartilage formation and mechanically stabilize of the fracture site by soft callus that gradually take on the appearance of cartilage. The formation of intramembranous bone tissue distal to the fracture area occurs by osteoblasts, which are gradually replaces the cartilaginous tissue through endochondral ossification resulting in formation of hard callus which increases the stability of the osteotomy or the fracture site (Lastayo *et al*., 2003).

Bone development requires complete vascularization, so it is not surprise that many growth factors have both mitogenic and angiogenic primary actions (Albrektsson and Johansson, 2001). Furthermore, replacements work in concert with growth factors to stimulate the cells recruitment, development, and differentiation progenitor cells of bone (Lauzon *et al*., 2012). The application of growth factors significantly accelerated the healing of fractures (Schmidmaier *et al*., 2002).

2.5.2.2.3 Remodeling phase

The third phase involves the formation and mineralization of the callus and replacement of the mineralized callus with mineralized bone and sculpting of the bone back to its original shape, size, and biomechanical competency via modeling and remodeling. This phase can also be referred to as secondary bone formation and involves converting the irregular woven bone callus into the lamellar bone. In this phase, osteoclasts resorb the newly woven bone and osteoblasts replace this matrix with the lamellar bone. The important functional outcome of the remodeling phase of fracture healing during homeostatic remodeling is the restoration of mechanical strength and stability (Oryan *et al*., 2015).

Osteoclasts become polarized and adhere to the mineralized surface and continue remodeling of bone. They form a ruffled border, which is sealed off and acid and proteinases are pumped into the resorption domain, and bone resorption by osteoclasts creates erosive pits on the bone surface known as ‘Howship’s lacuna.’ Once completed, osteoblasts are able to lay down new bone on the eroded surface (Schindeler *et al*., 2008).

Numerous pro-inflammatory signals, including IL -1, IL -6, and IL -11, as well as increased levels of TNF -α, IL -12, and interferon -γ (IFN -γ), control this remodeling phase. Parathyroid hormone and Growth hormone both play important roles in this stage, accelerating the fractured callus's repair and strengthening (Mountziaris and Mikos, 2008).

The callus's size must be large enough to compensate for the primitive bone’s relatively low strength, and bone lamellae must be aligned parallel to the longitudinal axis of the greatest force. Adequate loading is also necessary to promote osteogenesis and guide the ideal osteons geometric configuration, which will improve strength and stability at the site of fracture (Lastayo *et al*., 2003). Adequate strength may take six months to reach, and the remodeling phase can take months or even years (Pilitsis *et al*., 2002).

2.5.3 Fractures healing complications

The complications of fracture healing are classified into three groups:

2.5.3.1 Immediately complications

Injury to major vessels, injury to muscles and tendons, injury to joints injury to viscera (local) and hypovolemic shock (systemic) can be associated with fracture healing (Oryan *et al*., 2015).

2.5.3.2 Early complications

Septicemia in open fracture, aseptic traumatic fever, fat embolism syndrome, adult respiratory distress syndrome deep vein thrombosis, crush syndrome, pulmonary syndrome (systemic), infection, and compartment syndrome (local). This type of complication occurs during fracture treatment or immediately after treatment ends (Oryan *et al*., 2015).

2.5.3.3 Late complications

This type of complication can occur after a period of time from fracture treatment which include: delayed union, malunion, cross union and nonunion (imperfect fracture union) and osteonecrosis, shortening, sudeck's dystrophy, joint stiffness, osteomyelitis, ischemic contracture, osteoarthritis, and myositis ossificans. Another complication includes nerve damage, constant pain, wound problems and vascular injury that need a further surgical intervention (Allison *et al*., 2011).

2.6 Nanotechnology

The study of extremely small structures which defined as those smaller than 100 nm, is known as nanotechnology and it is generally regarded as nanoparticle (NPs). Due to their different electrical and physicochemical properties, the nanoparticles have more attention in the fields of biotechnology, electronics, aerospace engineering and the medical and agricultural field. According to their important contribution to the medical field NPs are mainly used as a drug new delivery system, DNA, monoclonal antibodies and proteins. The NPs are prepared from their bulk counterpart materials such as metallic and non-metallic, mono polymers etc., whereas, liposomes, polyethylene glycol and dendrimers are widely theragnostic using (Bahadar *et al*., 2016).

The main properties of the NPs which are the high surface area, solubility, small size, surface charge and multi functionality makes them unique. Due to their application in various fields these NPs have been used in clinical practice and medical researches employed for the diagnosis, treatment, monitoring and control of biological systems as it is known as nanomedicine. Many of the pharmacokinetic (PK) problems that may associate with many drugs that has been used in a variety of

disease classes can solved by the NPs by delivering of the therapeutic molecules, NPs have been proved as a carrier of drug.

There are different types of nanoparticles which can be used as delivery carriers of drug and therapeutic agents such as, liposomes, polymers dendrimers and metallic NPS such as selenium (Se), silicon (Si), titanium (Ti), silver (Ag), gold (Au), cerium (Ce), ferrous (Fe) and zinc (Zn) (Khurana *et al*.,2019).

2.7 Selenium (Se)

Selenium is an element whose present in trace amounts but it's essential for life and has gained a considerable attention in technical, human and agricultural fields of science due to its photoelectrical, piezoelectric and semiconducting properties. Selenium element is a key player in the control of reactive oxygen species (ROS) by action as an antioxidant and is known to regulation of many physiological processes, including cell differentiation and anti-inflammatory activities (Lee *et al*., 2021).

Selenium is very significant in the domains of biology, chemistry, and physics. Clinical research showed that the bones contain the second-highest proportion of selenium in the body (Zachara *et al*., 2001). deficiency of Selenium leads to degeneration of many tissues and organs, for example disorders related to joints, heart muscle, prostate cancer, thyroiditis and asthma (Kieliszek and Błażejak, 2016).

Selenium is found in nature in both forms: organic such as (selenocysteine and selenomethionine) and inorganic form as (selenate and selenite), also, selenium can be found in both crystalline and amorphous polymorphism forms (Zhu *et al*., 2019).

Globally, delays or failures in bone union pose a serious therapeutic problem. However, BMSCS have been suggested as a potentially effective treatment for accelerated bone fracture repair. Selenium has the ability to control BMSC differentiation and proliferation. Se-treatment inhibits the production and differentiation of the mature osteoclasts while promoting osteoblastic development of BMSCs (Li *et al*., 2019).

2.8 Selenium Nanoparticles (Se-NPs)

In mammals, at least 30 seleno-proteins have been identified in the body tissue and it has been found that play important roles in the body (Majeed *et al*., 2018), seleno-proteins containing selenium in the form of selenocysteine which are critical for bone remodeling (Kim *et al*., 2021). In comparison to inorganic and organic selenium molecules, nano selenium has greater bioavailability and biological activity (Kondaparthi *et al*., 2019). Se-NPs are considered to be healthier and less toxic when compared with many metal-based nanomaterials due to the generation of reactive oxygen species from another metals, especially heavy metals (wang, 2015). Se-NPs have possessed catalytic activities with its bioactivity (Cavalu *et al*., 2018).

Because metals, especially heavy metals, produce reactive oxygen species, Se-NPs are thought to be safer and less harmful than many metal-based nanomaterials, and when are compared to their elemental form, researchers discovered that the Se-NPs are less toxic than the elemental form. For instance, in a previous studies conducted on mice, it is found that the LD50 of seleno-methionine is 25.6 mg Se/kg, whereas the Se-NPs' LD50 was 92.1 mg Se/kg. (Wang *et al*., 2007).

Se-NPs are characterized by having high bioavailability and several therapeutic effects owing to their anti-inflammatory, antioxidant and neuroprotective and for treatment of an inflammation-mediated diseases, including cancer, nephropathy, diabetes and arthritis (Kondaparthi *et al*., 2019; Liu *et al*., 2022), also act as anticonvulsant to prevent neuronal loss by oxidative damage (Yuan *et al*., 2020).

The Se-NPs have been used for the medical purposes such as antimicrobial uses for inhibition of bacterial growth (Tran and Webster, 2011), also it can be used as osteo-inductive by promote mesenchymal stem cells differentiation to osteoblast (Fatima *et al*., 2021). Se-NPs promotes osteogenic differentiation of bone marrow mesenchymal stem cell and migration of cells to fracture site to accelerate bone fracture healing (Li *et al*., 2019), also used to prevention and treatment of osteoporosis (Li *et al*., 2023; Zhou *et al*., 2023). Se-NPs can be used to enhance adhesion of osteoblast to play a role of anticancer in orthopedic application (Tran *et al*., 2008). A medication may be transported to the site of action by the Se NPs which acting as a carrier (Kondaparthi *et al.*, 2019).

Se-NPs can be used in coating of implant to prevent infection of bone (Tran *et al*., 2019; Alheeti and Fatalla, 2021). The Se-NPs can be used for cranioplasty by coating of titanium mesh (Cavalu *et al*., 2018), also, Se-NPs have an antifungal property (Lara *et al*., 2018). The use of Se-NPs as clear indicators of hepatotoxicity is thought to mitigate the liver damage that caused by high doses of Se. When Se-NPs are coupled to distinct Se species (selenite, organic selenium and selenium), they can display increased anticancer efficacy and decreased toxicity (Kondaparthi *et al.*, 2019).

2.8.1 Se-NPs synthesis

Se-NPs are synthesized through three types of methods which are: chemical methods, physical methods and the biological methods.

2.8.1.1 Chemical methods

This less safe approach of synthesizing selenium nanoparticles included the use of high temperatures, hazardous chemicals, and an acidic pH for the catalytic reduction of ionic selenium (Wadhwani *et al*., 2016; Gunti *et al*., 2019).

2.8.1.2 Physical methods

The using of pulsed laser ablation (PLA) or deposition consider one of the physical methods for Se-NP creation (Quintana *et al*., 2002) such as, phyto-thermal associated synthesis, electrodeposition techniques and microwaves synthesis and these methods of synthesis are less common use than the chemical methods (Quester *et al*., 2013).

2.8.1.3 Biological method

The most effective method for Se-NP creation is the biological methods, on which yeast, algae, fungi and plants are used as biological catalysts for nanoparticles synthesis. Because of its lower cost, fast growth rate of microorganisms and plants, lower toxicity, common procedures for culturing, and eco-friendly production of nanoparticles it is consider advantageous over the other two methods (Quester *et al*., 2013; Murugesan *et al*., 2019).

Chapter Three

Materials and Methods

3.1 Ethical approve

The experimental design has received approval from the institutional animal care and use committee at the College of Veterinary Medicine, Mosul University under the registration number UM.VET.2023.105.

3.2 Experimental animals

24 clinically healthy adult male dogs have been used in the experimental study, weighing (25 ± 0.5) kg and aged (2 ± 0.5) years Animals were examined clinically before the experiment is conducted, to ensure that they are free from diseases. The experimental animals housed separately (every animal in one cage) in the animal house of the College of Veterinary Medicine in the University of Mosul. A subcutaneously injection of ivermectin 1% (vermectin, vapco, Jordan) at a dose of (0.2 mg/kg) is given to control the external and internal parasite if present. Before the operation, animals are left in their cages two weeks for adaptation and they provided feed, water according to the same institutional protocol. Animals are monitored all over the periods of experiment and all data are recorded.

3.3 Experimental design

The experimental animals were divided randomly into two equal groups (n= 12):

1. First group (control group): On which a transverse fracture was made in the distal radial part using wire saw and the fracture site leaved without adding any material, then reduction and fixation by fiber glass cast tape was done.
2. Second group (treated group): On this group as in the first group a transverse fracture was made, then treated by pour with selenium nanoparticles (Se-NPs) on the fracture line, reduction and fixation by fiber glass cast tape was done. Then follow-up evaluation was acheived by using clinical, radio-graphical, histological and histochemical evaluations on 2, 4, 6 and 8 weeks post-operation as show in (Figure 3).

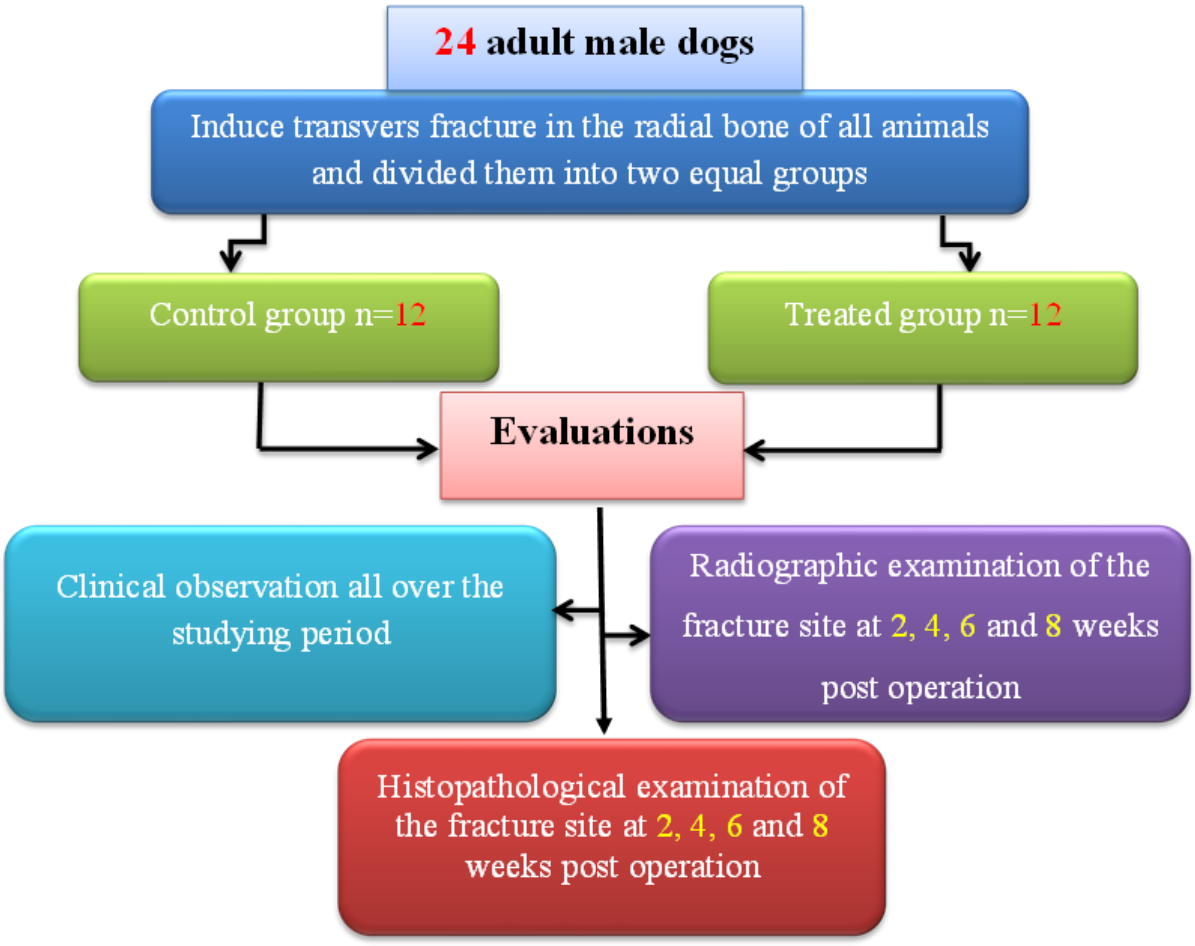

Figure 3.1 Photographic images show the Illustration of the experimental design of the study.

3.4. Selenium nanoparticles

3.4.1 Evaluation of selenium nanoparticles

One of the evaluations methods for Se-NPs identification and determination the grain size is the X-ray diffraction analysis (XRD) as shown in figure 3.2 according to (Saeed *et al*., 2019).

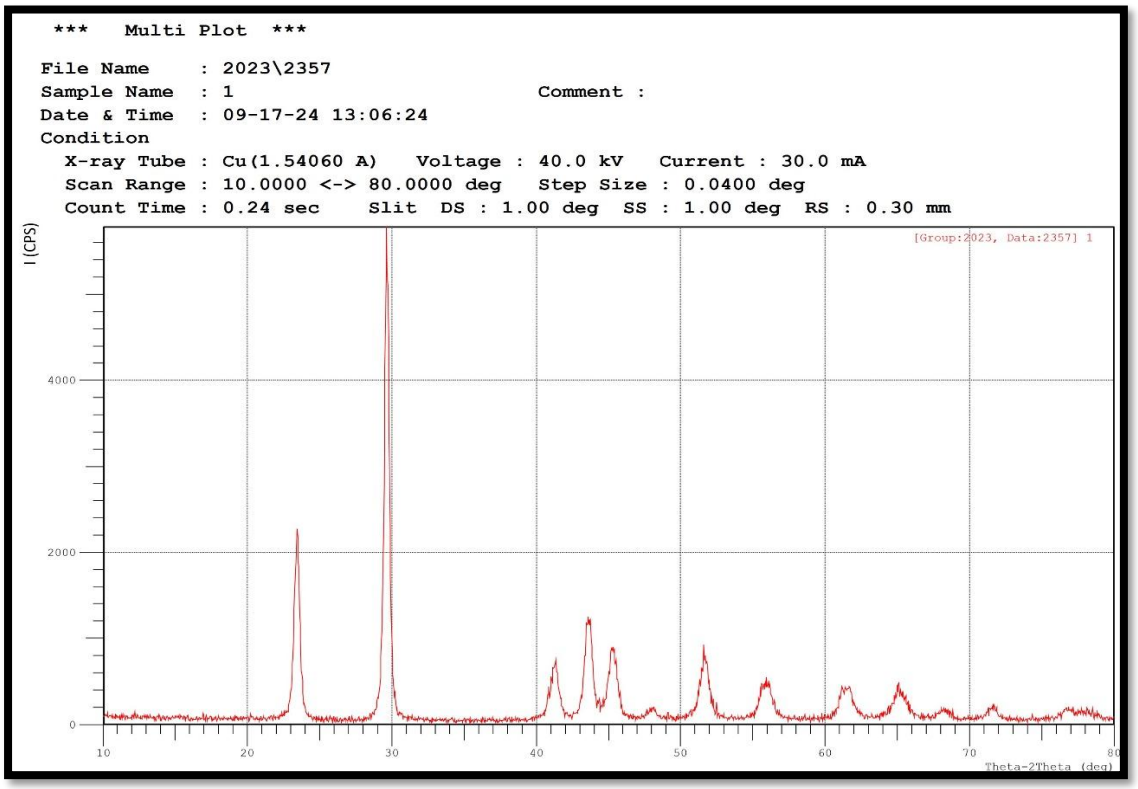

Figure 3.2 Photographic images show XRD pattern of selenium nanoparticles.

3.4.2 Preoperative nano-selenium preparation

The preparing of nano selenium for operation has been done by using a sensitive balance to weight 1250 µg from nano-selenium powder (50 nm, Sigma Aldrich company, USA) on test tube, then adding to the weighted powder 10 ml of distilled water, and by shaking the test tube a suspension of selenium nanoparticles was obtained at a dose of 125 µg/ml (El-Sayed *et al*., 2023) which was placed around the fracture site.

3.5 Surgical procedures

3.5.1 Anesthesia

The surgical operations of all dogs have been conducted under general anesthetic protocol which is done using of a mixture containing 10% ketamine HCL (Alfasan, Holand) at doses (15 mg/kg) and xylazine HCL 2% (Nita Farm, Russia) at doses (5 mg/kg) through intramuscular injection (Mohammed *et al.*, 2022).

3.5.2 Surgical operation

The site of operation is prepared for aseptic surgery from elbow joint to the carpal joint by clipping and shaving, then restrain the animal at lateral recumbency on the right side with extension of right limb foreword and the left limb pulled posteriorly to give best surgical approach, then the head, neck, shoulder and right forelimb is covered with surgical towels except the operation site leaved open (Figure 3.3A). Povidone-iodine solution 10% (Sakaria, Turkey). was used as antiseptic on the site of operation. Skin incision is performed about 4-5 cm in length by surgical blade (size 22) in cranio-medial approach which consider the best site to reach the distal extremity of the radius bone with low invasiveness (Thanoon *et al*., 2019; Thanoon, 2019), then blunt dissection of subcutaneous fascia and connective tissue are done by blunt ends surgical scissor and curved hemostatic forceps to separate and display the radial bone (Figure 3.3B). After reaching the radius bone the common digital extensor tendon is separated and pulled out by using towel clamp to prevent iatrogenic tenotomy during radial fracture creation by wire saw (Figure 3.3C). Wire saw is inserted around the radial bone by using curved hemostatic forceps and suture material surgical needle which

passed around the bone and pulled the connected wire saw (Figure 3.3D), and by moving the wire saw around the bone a transvers fracture is conducted (Figure 3.4A).

In the control group, the fracture site is left without any addition and the muscles and subcutaneous tissue are closed by simple continuous pattern using polyglycolic acid suture (No. 1) (Yingmed, China), then skin is closed by simple interrupted technique using silk suture (No. 2) (Greetmed, China). External fixation by using fiber glass cast tape (size No. 3) (Jiangsu Senolo Medical Technology Co., Ltd, China) is done with leaving an open window above the site of operation for daily wound dressing by povidone-iodine solution 10%.

While in treated group, 1 ml of selenium nanoparticles suspension at a dose of (125 µg/ml) is applied at the fracture site (Figure 3.4B), then muscles, subcutaneous tissue and skin are closed by same method like in the control group (Figure 3.4C). External fixation with fiber glass cast tape is also done as in control group (Figure 3.4D).

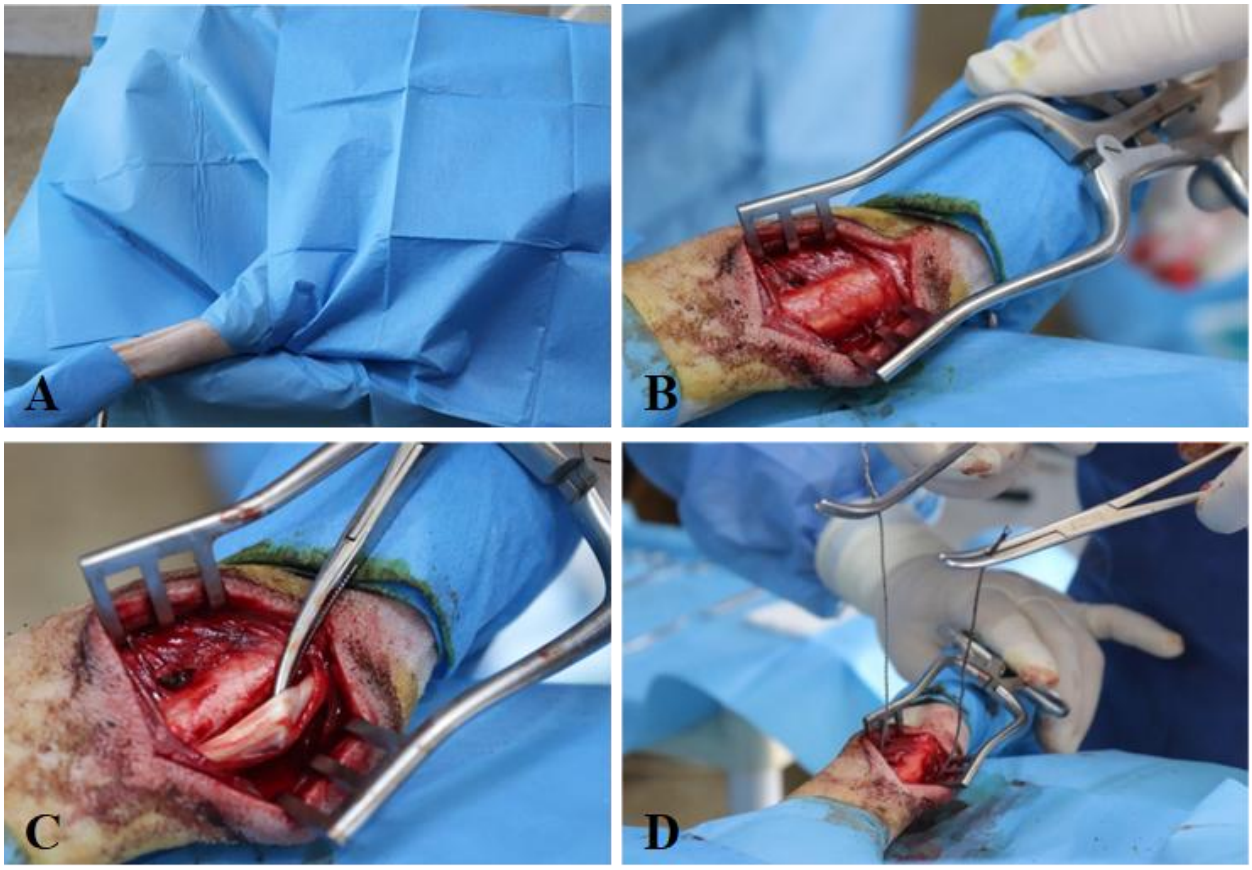

Figure 3.3 Photographic images show (A)preparing the site of operation, (B) the distal part of radial bone, (C) separation of tendon from radial bone, (D) insertion of wire saw around the radial bone.

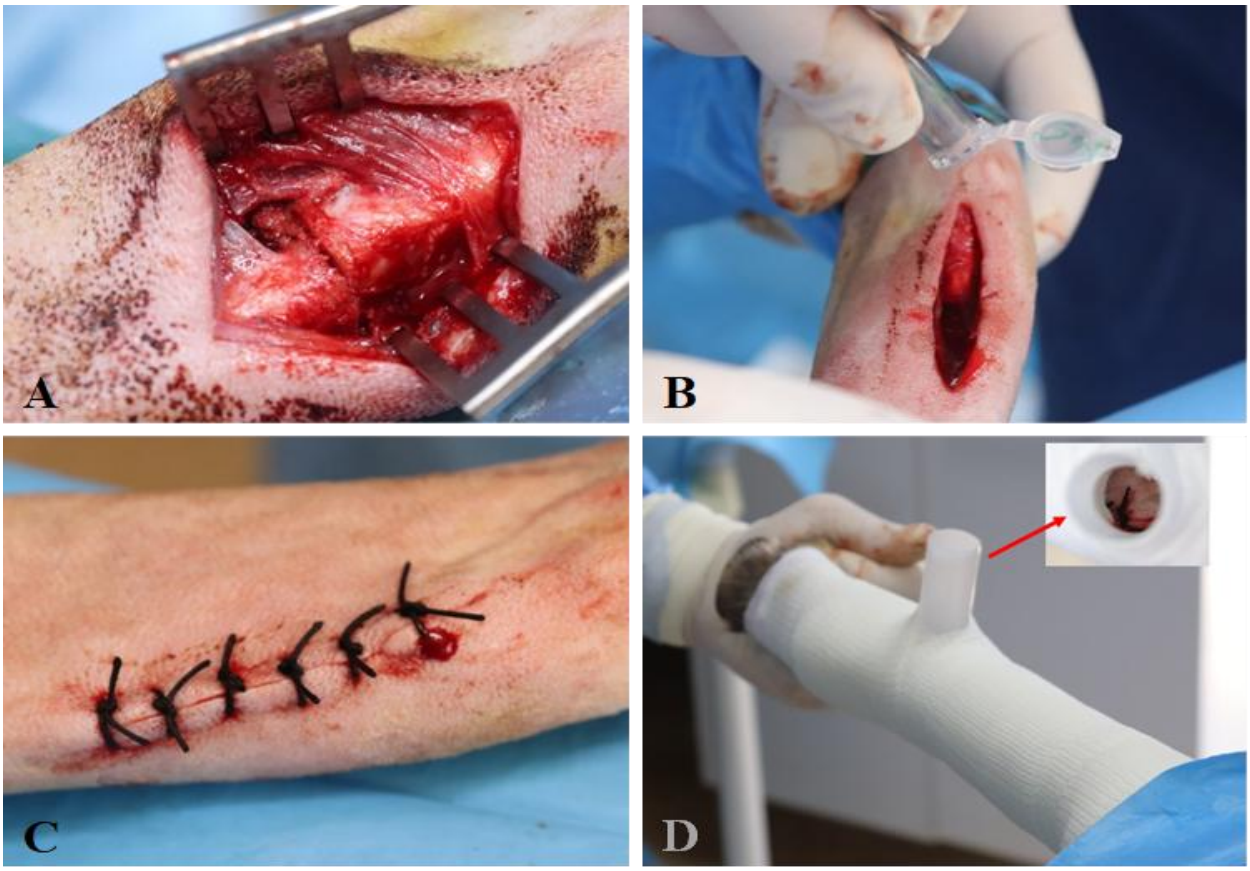

Figure 3.4 Photographic images show (A) transverse radial bone fracture, (B) application of nano-selenium suspension around the fracture site, (C) closer of skin with silk using simple interrupted pattern, (D) placing of fiber glass cast tape with window over the operation site.

3.6 Postoperative care

After surgical operation, the animals were observed and monitored for the entire duration of the 8-weeks study. All dogs are submitted to postoperative protocol by injection of analgesics drugs like dipyrone (Uvedco, Jordan) at a dose of (25 mg/kg) intramuscularly for five days to relieve the pain (Silva *et al*., 2021), and injection of penicillin-streptomycin (Pensrep, Interchem, Holand) intramuscularly as broad-spectrum systemic antibiotic at a dose of (Penicillin 10,000 IU-Streptomycin 15 mg/kg) for five consecutive days. The skin wound is managed through fiber glass cast window with local application of 10% povidone-iodine solution two time daily for 5-7 consecutive days to prevent infection of the wound.

3.7 Experimental evaluations

The effect of selenium nanomaterial on the fracture healing is evaluated clinically, histopathological and radiographically.

3.7.1 Clinical evaluations

All dogs in both groups have been monitored daily in first week, then intervals every week to check any abnormal change in the life signs such as appetite, pain signs, gate and weight bear on the fractured limb by grades application of visual assessment of gait according to (Carr and Dycus, 2016) which described in (Table 3.1).

Table 3.1 Example of a Numerical Rating Scale for Visual Assessment of Gait.

Lameness Grades	Description
Grade 1	Sound at the walk, but weight shifting and mild lameness noted at trot
Grade 2	Mild weight-bearing lameness noted with the trained eye
Grade 3	Weight-bearing lameness, typically with distinct “head bob”
Grade 4	Significant weight-bearing lameness
Grade 5	Toe-touching lameness
Grade 6	Non–weight-bearing lameness
Note:	Grades 2 through 6 lameness can be observed at the walk or trot.

3.7.2 Radiographical evaluations

Immediate post-operative radiographic assessment of the fractured bone was conducted utilizing standardized mediolateral and craniocaudal X-Ray projection to evaluate the adequacy of fracture reduction and alignment. Subsequent serial radiographic evaluations were performed at 2, 4, 6 and 8 weeks post-operatively to monitor fracture healing progression, assess callus formation and evaluate the integrity of the fracture union, utilizing plain radiography imaging modalities. All radiographic images were acquired using computed radiography (CR) technique, which provides high-resolution digital images with enhanced diagnostic accuracy. Radiographic images taken in X-ray room in the University Veterinary Hospital using the plain X-ray machine (Shimadzu, Japan) accompanied by the digital wireless detector (Italray, Italia) with exposure factors seated at 58 kV, 3.2 mAs and 90 cm focal-film distance (FFD) to estimate the bone healing stages of the fractured bone.

3.7.3 Histopathological evaluations

The bone biopsies collection has been conducted at intervals of 2, 4, 6 and 8 weeks post operations from all experimental animals, then fixed by neutral buffer formalin (NPF) at concentration of 10% for 72 hr., then all samples are submitted to decalcification by formic acid to facilitate the following series processes of histological techniques which are start with fixation in neutral buffer formalin (NPF) at concentration of 10%, then dehydration by different concentrations of alcohol(50%, 70%,90% and 100%), then clearing by using xylene, then embedding in paraffin wax, then cutting by microtome, then put the section in water path to facilitate mounting on slide, then using of xylen to remove paraffin wax, then dehydration by different concentrations of alcohol, then staining by both routine staining (hematoxylin and eosin) and special staining (Masson Trichrome and Alizarin / Alcian blue) (Suvarna *et al*., 2018). The histological sections were analyzed based on semi-qualitative system as shown in (Table 3.2). A descriptive catalog was designed to estimation of the histochemical staining by Masson Trichrom as shown in (Table 3.3).

Table 3.2 Semi-qualitative analysis of radius bone fracture healing.

Score-Grade	Osteogenic Matrix	Osteoclast Number / Fields
+ / **Mild**	Few components of both osteo-connective tissue and adipose tissue, fibroblast and blood vessels	1-5
++ / **Moderate**	Moderate component of both osteo-connective tissue and adipose tissue, fibroblast and blood vessels	10-15
+++ / **Sever**	Abundant component of both osteo-connective tissue and adipose tissue, fibroblast and blood vessels	≥ 25

Table 3.3 Histochemical analysis of Masson Trichrom stain.

Score	Bony callus levels
+	Few < 5 % bony tissue / field
++	Equal to 30-40% bony tissue / field
+++	More than 60-80% bony tissue / field

3.8 Statistical analysis

Computer package (Sigma plot V12.0 / SYSTAT software) has been used to conduct the parameter analysis. Data have been presented as means ± standard error (SE) and were analyzed using one-way analysis of variance (ANOVA) and t-test with the significant level set on $P \leq 0.05$ and the differences among the groups are determined by Duncan's multiple range test (Petrie, 2013).

Chapter Four

Results

4.1 Clinical evaluations

The experimental animals in both groups have been monitored daily for first two weeks post operation, then in interval every week which has showed tenderness in the first and second day with partial loss of appetite then gradually return to the normal appetite.

Assessment of experimental animal's gait post operation that showed the following: At the 1st week the control group observed disuse of the fractured limb with non-weight-bearing lameness occupy grade VI, while the treated group start to touch the ground with the affected limb with lameness occupy grade V. At the 2nd week the control group start to touch the ground with lameness occupy grade V, while the treated group appeared significant weight bear with lameness occupy grade IV. At the 3rd week the control group starts to weight bear significantly with lameness occupies grade IV, while the treated group appeared weight bearing lameness with head bob which occupy grade III. At the 4th week the control group still weight bear significantly wit lameness occupies grade IV, when the treated group appeared mild weight bearing lameness occupy grade II. At the 5th week the control group showed weight bearing lameness with head bob which occupy grade III, while the treated group still mild weight bearing lameness occupy grade II. At the 6th week the control group showed weight bearing lameness with head bob which occupy grade III, while the treated group showed mild lameness at trot which occupy grade I. At the 8th week the control group occupy grade II, while the treated group occupy grade I as show in (Table 4.1).

Table (4.1) Show the grades of lameness in the two group of the experimental animals.

Fracture / weeks	Groups	Grades
1	Control group	6
	Treated group	5
2	Control group	5
	Treated group	4
3	Control group	4
	Treated group	3
4	Control group	4
	Treated group	2
5	Control group	3
	Treated group	2
6	Control group	3
	Treated group	1
8	Control group	2
	Treated group	1

4.2 Radiographical evaluations

The radio-graphical investigation has been conducted of all experimental animals at intervals (2^{nd}, 4^{th}, 6^{th} and 8^{th}) weeks post-operation to estimation the degree of fracture healing that showed the following:

In the control group at the second week post-operation the fracture line was clear, radiolucent and with only small amount signs of periosteal reaction, while the treated group shows clear periosteal reaction around the fracture site with fracture line appearance (Figure 4.1) and (Figure 4.2).

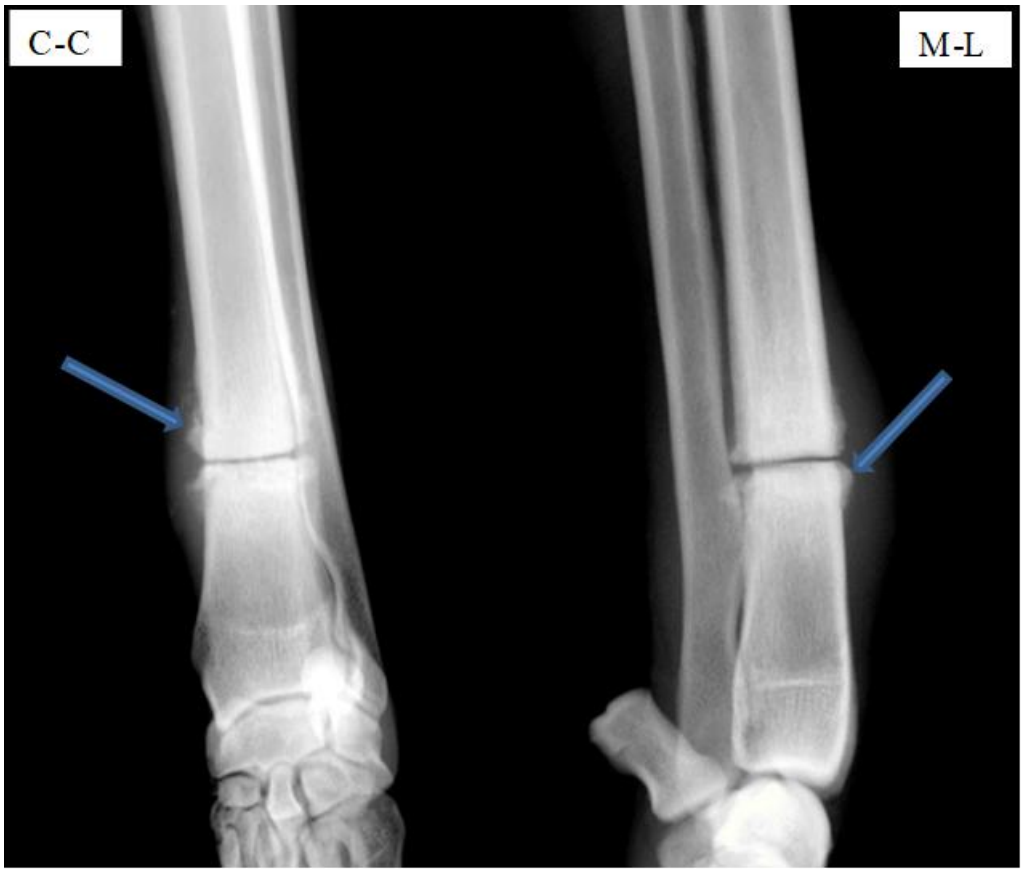

Figure 4.1 Radiographic image shows cranio-caudal (C-C), mediolateral (M-L) view of radial bone at 2nd week post operation in control group shows minimal periosteal reaction of the proximal and distal radial fracture segment (arrow) with clear fracture line.

Figure 4.2 Radiographic image shows cranio-caudal(C-C), mediolateral (M-L) view of radial bone at 2nd week post operation in treated group shows clear periosteal reaction around the fracture site (arrow) with fracture line appearance.

At the 4th week post operation of control group showed increase of periosteal reaction but the fracture line tile clear and begins to form of bridge callus while the treated group shows good periosteal reaction around the fracture site that bridges the line of fracture with blur of the fracture line's appearance (Figure 4.3) and (Figure 4.4).

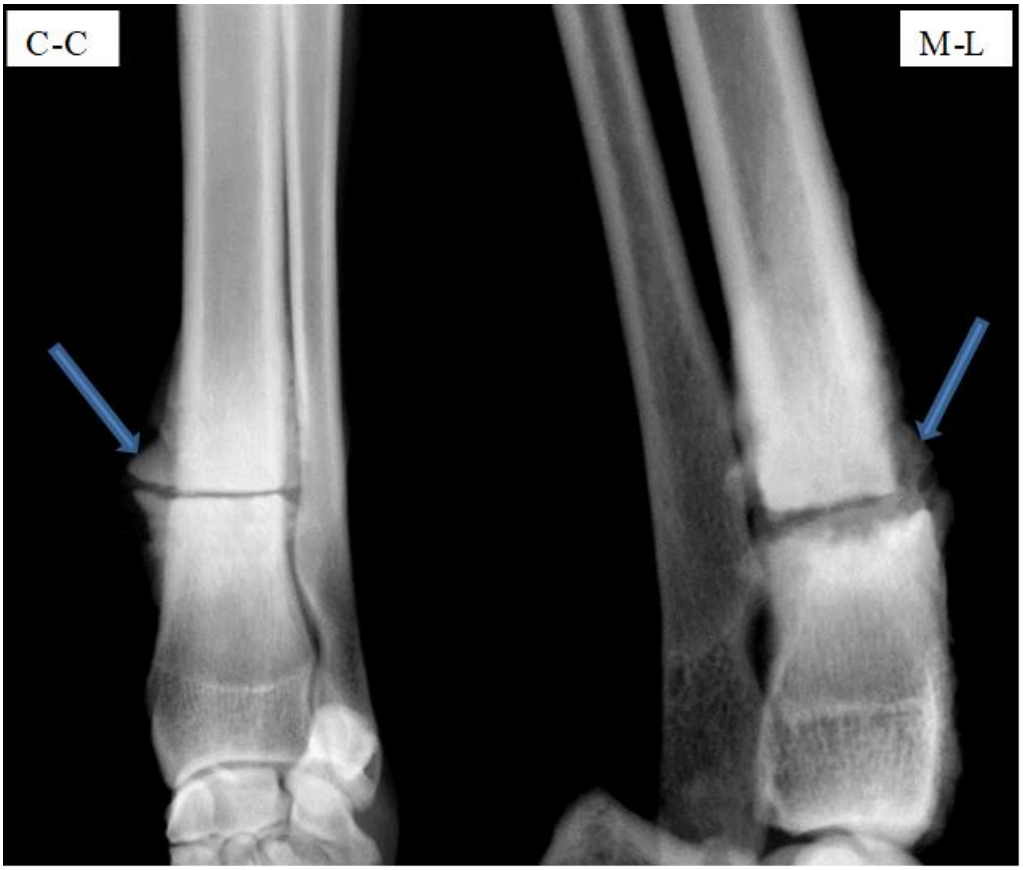

Figure 4.3 Radiographic image shows cranio-caudal (C-C), mediolateral (M-L) view of radial bone at 4th week post operation in control group shows increase periosteal reaction around the fracture site (arrow) with appearance of fracture line.

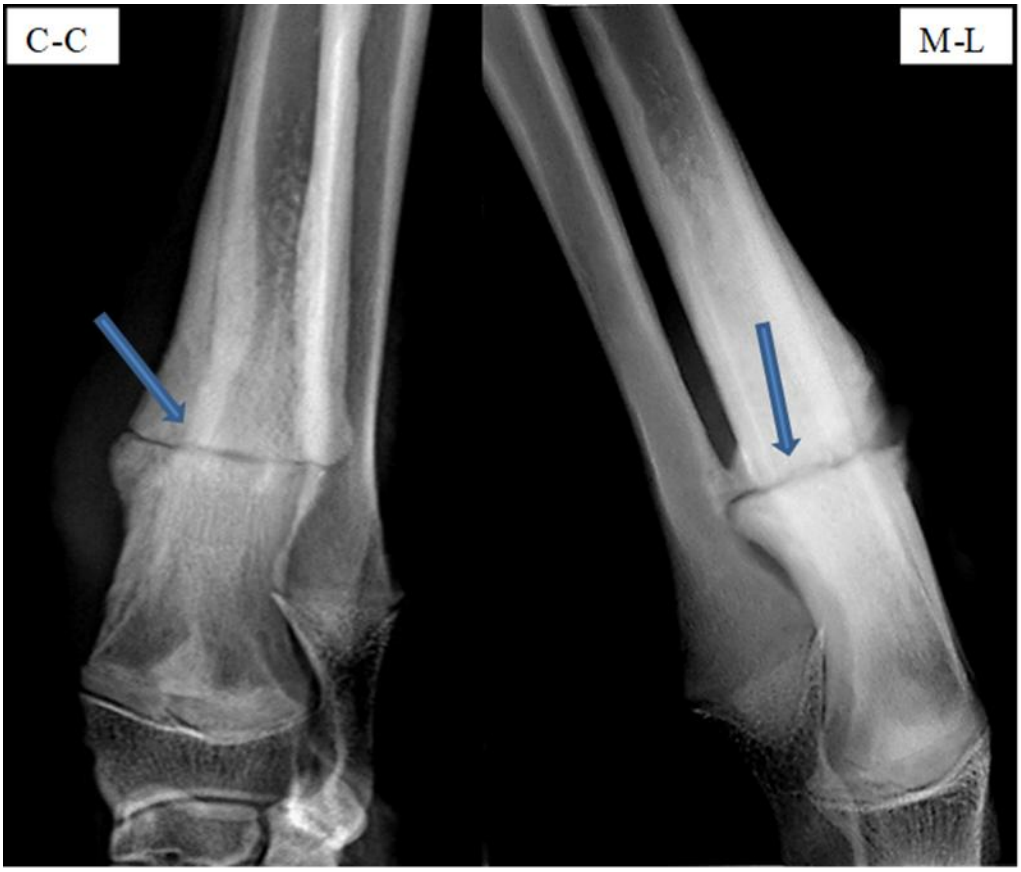

Figure 4.4 Radiographic image shows cranio-caudal (C-C), mediolateral (M-L) view of radial bone at 4th week post operation in treated group shows good periosteal reaction around the fracture site that bridges the line of fracture (arrow) with blur of the fracture line's appearance.

At the 6th week post-operation, the control group shows periosteal reaction and traces of callus formation in fracture site with moderate bridging of the hard callus growth and still appearance of fracture line, while in treated group shows more prominence periosteal reaction, there is an excellent hard callus formation that connects both fracture ends with no sign of the fracture line appearance of fracture site, and semi normal medullary canal appearance (Figure 4.5) and (Figure 4.6).

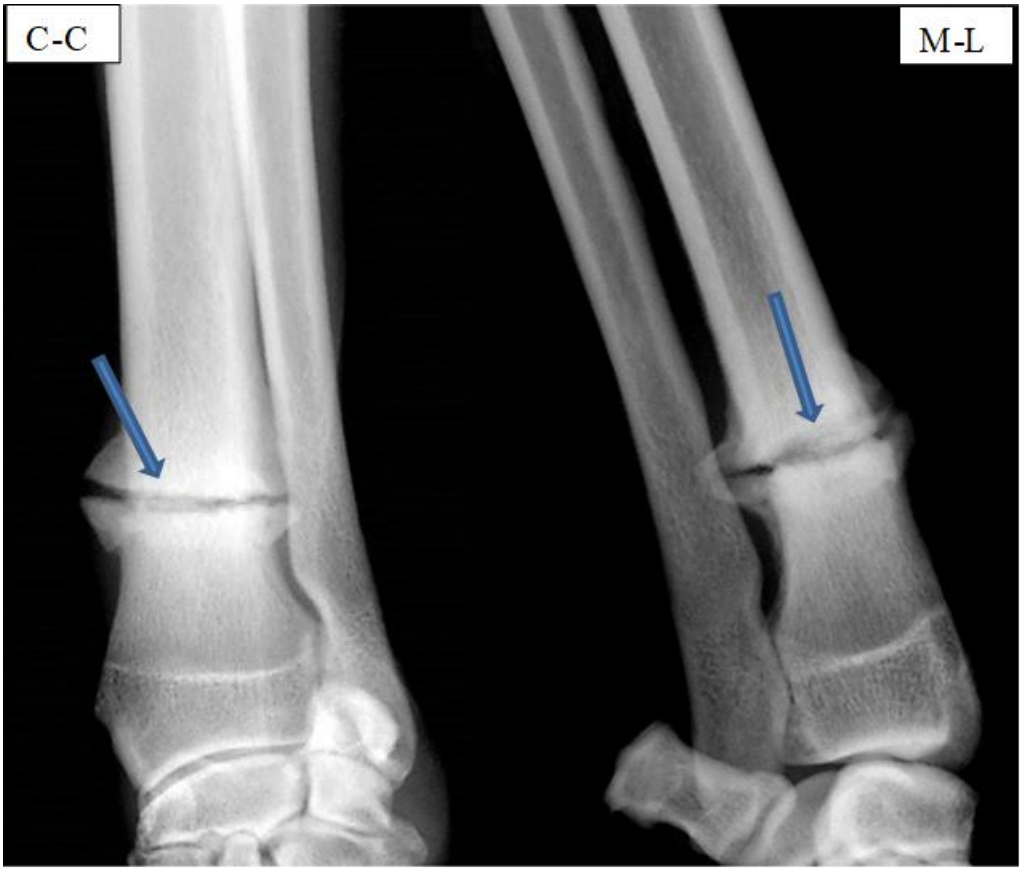

Figure 4.5 Radiographic image shows cranio-caudal (C-C), mediolateral (M-L) view of radial bone at 6th week post operation in control group shows periosteal reaction and traces of callus formation in fracture site with moderate bridging of the hard callus growth (arrow) and still appearance of fracture line.

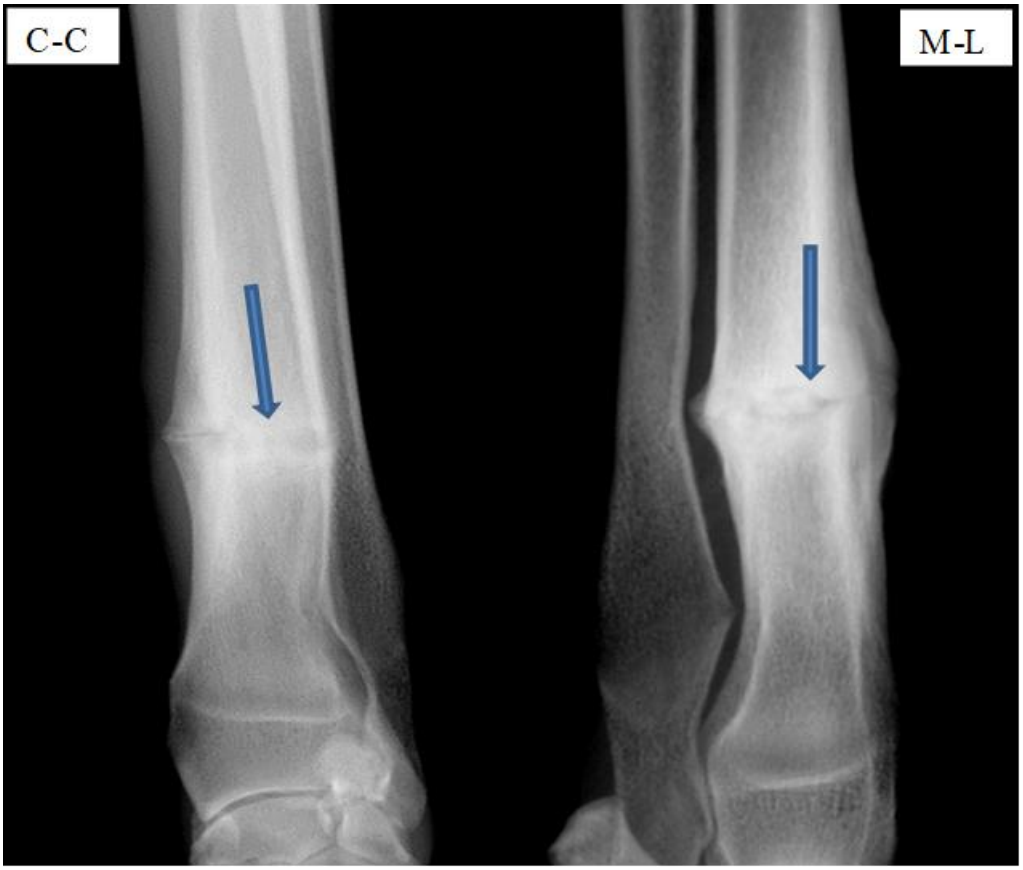

Figure 4.6 Radiographic image shows cranio-caudal (C-C), mediolateral (M-L) view of radial bone at the 6th week post operation in treated group shows more prominence periosteal reaction, there is an excellent hard callus formation that connects the fracture two ends with no sign of the fracture line appearance of fracture site (arrow), and semi normal medullary canal appearance.

At the 8th week post operation, the control group shows radio-opacity of callus formed at the fracture site which connect the fracture two ends and increase fracture line disappearance, while the treated group shows a decrease in the size of callus around the fracture site with reconnecting of the medullary canal and the bone appear as its normal shape (Figure 4.7) and (Figure 4.8).

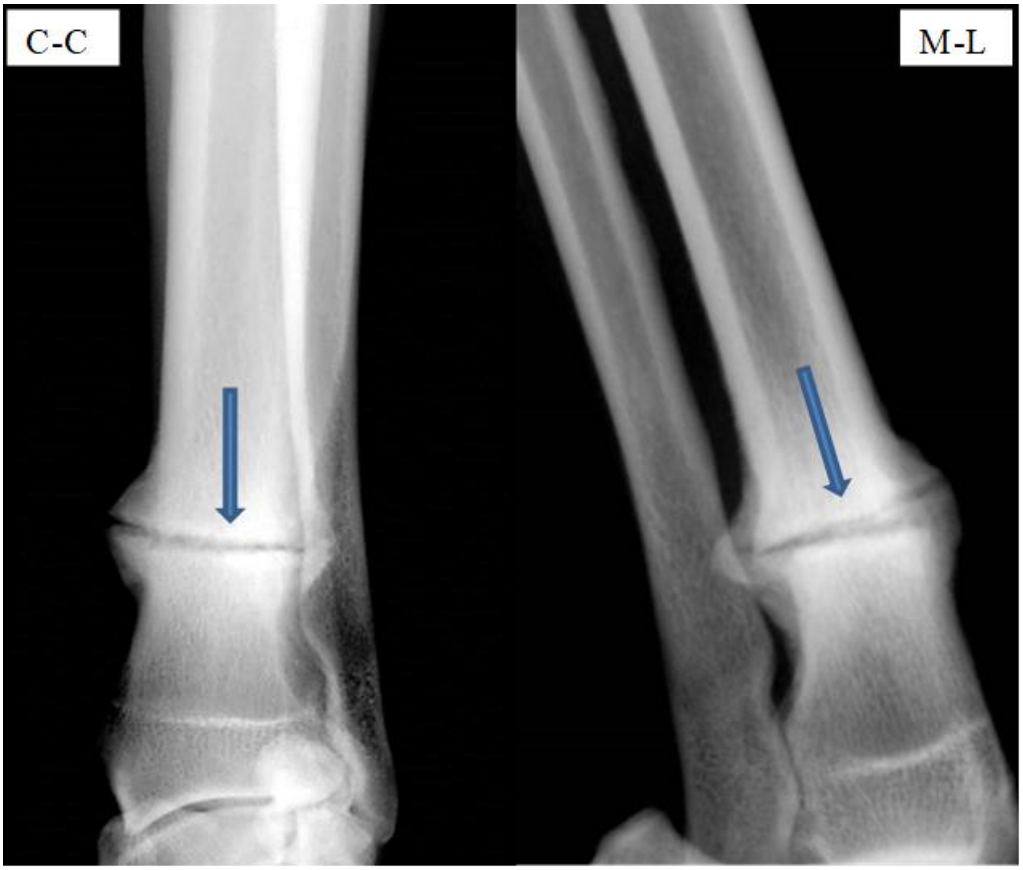

Figure 4.7 Radiographic image shows cranio-caudal (C-C), mediolateral (M-L) view of radial bone at the 8th week post operation in control group shows radio-opacity of callus formed at the fracture site which connect the fracture two ends (arrow) and increase fracture line disappearance.

Figure 4.8 Radiographic image shows cranio-caudal (C-C), mediolateral (M-L) view of radial bone at 8th week post operation in treated group shows decrease callus around the fracture site with reconnecting of the medullary canal and the bone took its semi natural shape.

4.3 Histopathological evaluations

The histopathological result of the biopsies taken from the distal radial fracture site in both groups (control and treated group) shows histopathological changes which are considered as indicator for healing, the different in pathological changes depend on post operation time at intervals of 2, 4, 6 and 8 weeks and also depend on groups.

On the 2nd week, histological examination of the radial fracture biopsy of the control group shows fibrous connective tissue with proliferative fibroblast and newly blood vessels (Figure 4.19), in other

section the histological examination reveal fibrocartilaginous callus formation (Figure 4.10), the microscopic examination investigated intra-cartilaginous bone (Figure 4.11) as well as irregular and thin woven bone around fracture border (Figure 4.12) formed of mild primitive osteon containing sever osteoclast and moderate irregular and disorganized osteocyte as in table (4.1).

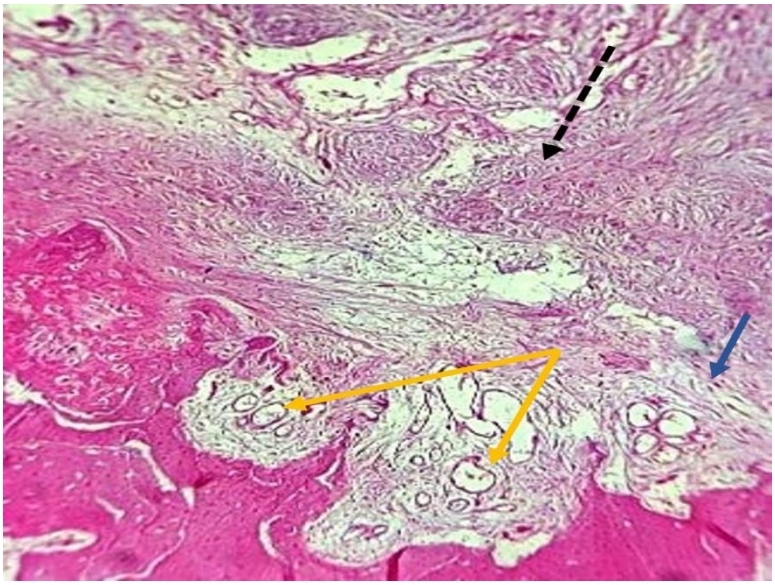

Figure 4.9 Histopathological findings in control group at 2nd week post operation show fibrous connective tissue (black–dash arrow), proliferative fibroblast (blue arrow) and newly blood vessels ± (yellow arrow), H&E, 100X.

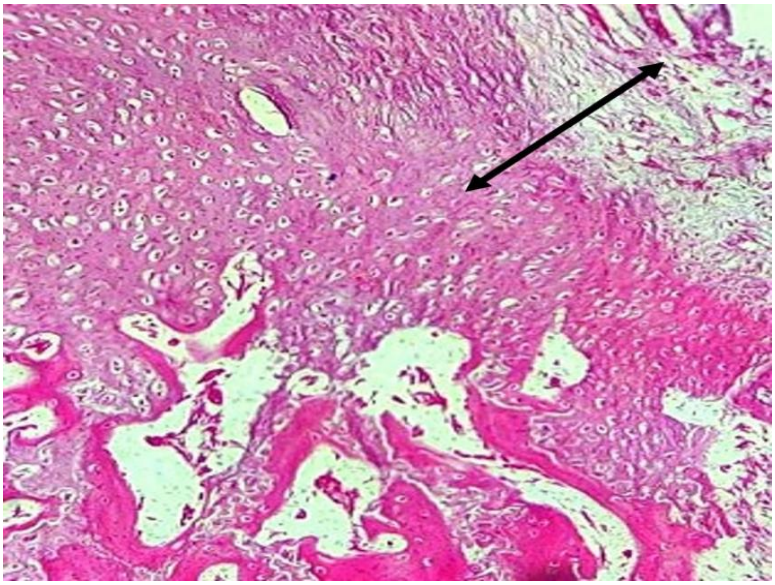

Figure 4.10 Histopathological findings in control group at 2nd week post operation show fibrocartilaginous callus (black two head arrow), H&E, 100X.

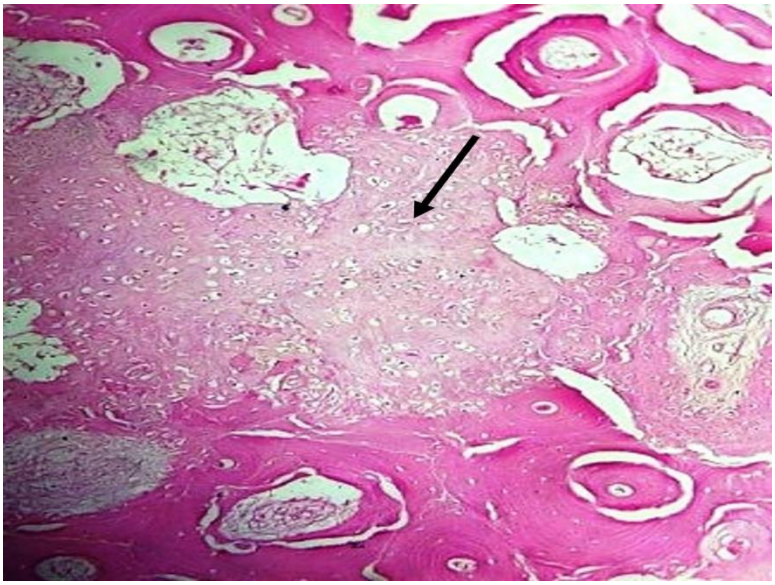

Figure 4.11: Histopathological findings in control group at 2nd week post operation show intra cartilaginous bone (black row), H&E, 100X.

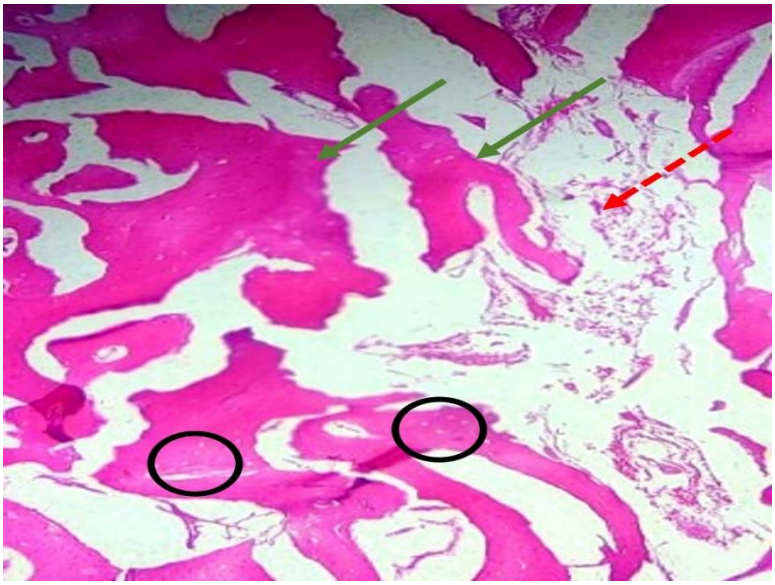

Figure 4.12 Histopathological findings in control group at 2nd weeks post operation show irregular thin woven bone (green arrow), mild primitive (red-dash arrow) and irregular dis organized osteocytes (black circles), H&E, 100X.

While the histological results of treated group showed regenerated bone represented by intra cartilaginous bone (thin channels) in greater amount, with newly formation of haversian canal furthermore moderate in score (++), primitive osteo matrix is formed in the center (Figure 4.13), there is small discrete islands enclosing osteocytes and lined with osteoblasts and osteoclasts proliferative occupy score (++) and moderate grade (Figure 4.14), table (4.1), as well as there is sever proliferative of chondroblasts and intense newly blood vessels formation (Figure 4.15)

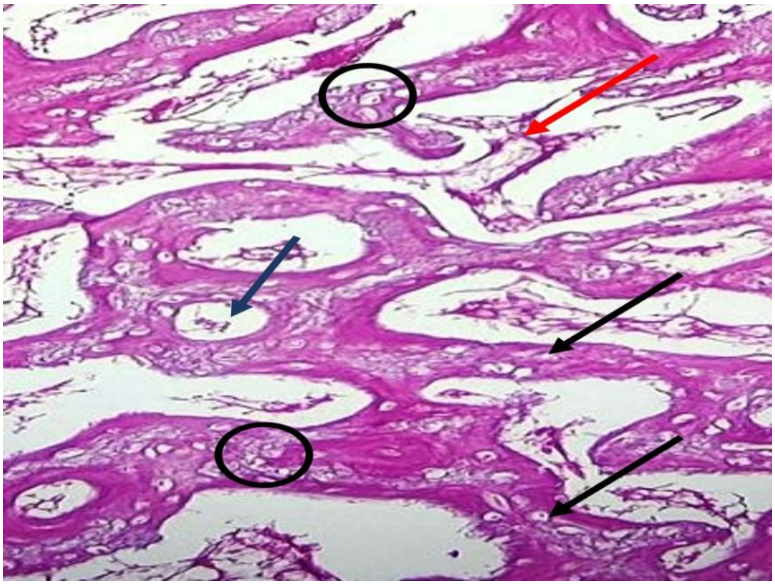

Figure 4.13 Histopathological findings in treated group at 2nd week post operation show great amount of intra cartilaginous bone (thin channels) (black arrow), newly haversian system formation (blue arrow), with moderate osteogenic matrix (red arrow), sever proliferative of chondroblast (black circles), H&E, 100X.

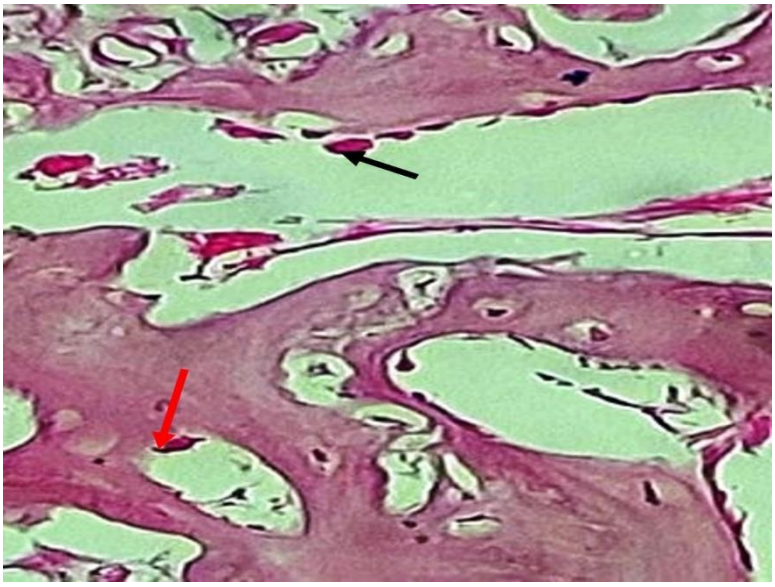

Figure 4.14 Histopathological findings in treated group at 2nd weeks post operation show moderate grade for both osteoblast (black arrow) and osteoclast (red arrow), H&E, 400X.

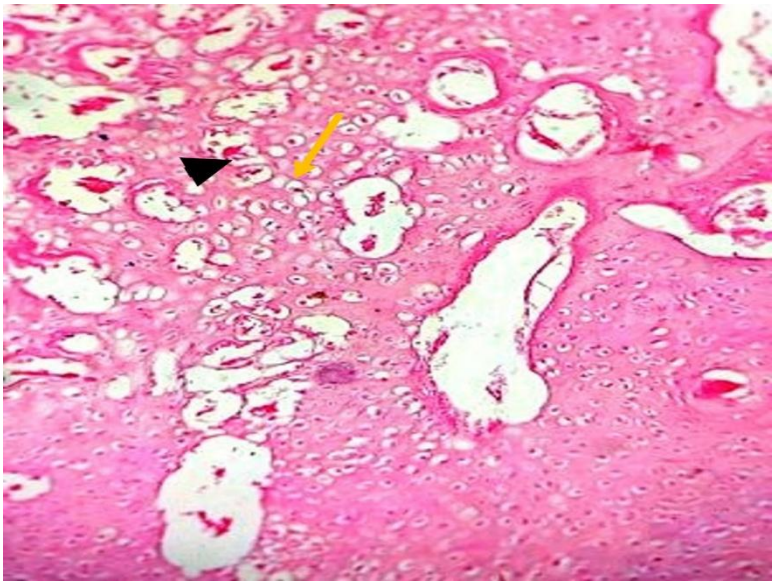

Figure 4.15 Histopathological findings in treated group at 2nd week post operation show intense newly blood vessels (black head arrow) and sever proliferative of chondroblasts (yellow arrow), H&E, 100X.

At the 4th week, histological investigation of the distal radial fracture site of the control group has showed that irregular and thicker trabeculae with moderate for both osteogenic matrix and proliferative of osteoclasts and these trabeculae include osteocytes and osteoblast, calcified trabeculae (Figure 4. 16 and figure 4.17), respectively.

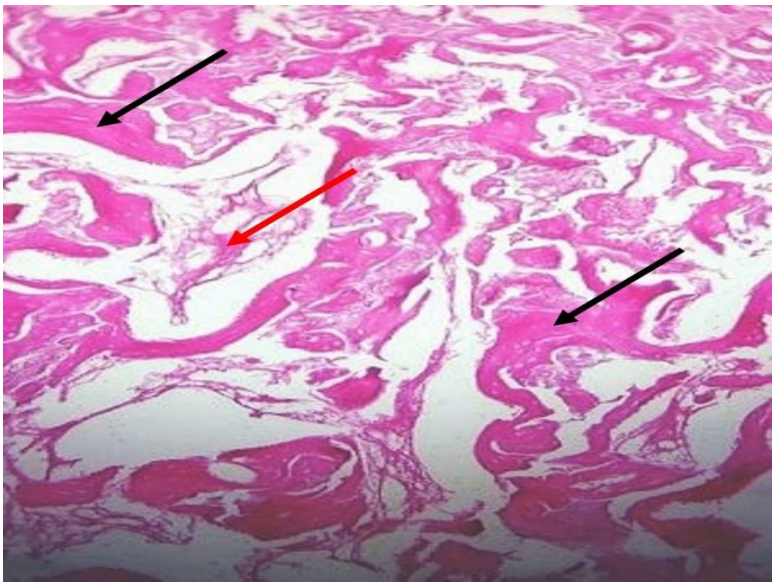

Figure 4.16 Histopathological findings in control group at 4th week post operation show irregular thick trabeculae (black arrow) with moderate osteogenic matrix (red arrow), H&E, 100X.

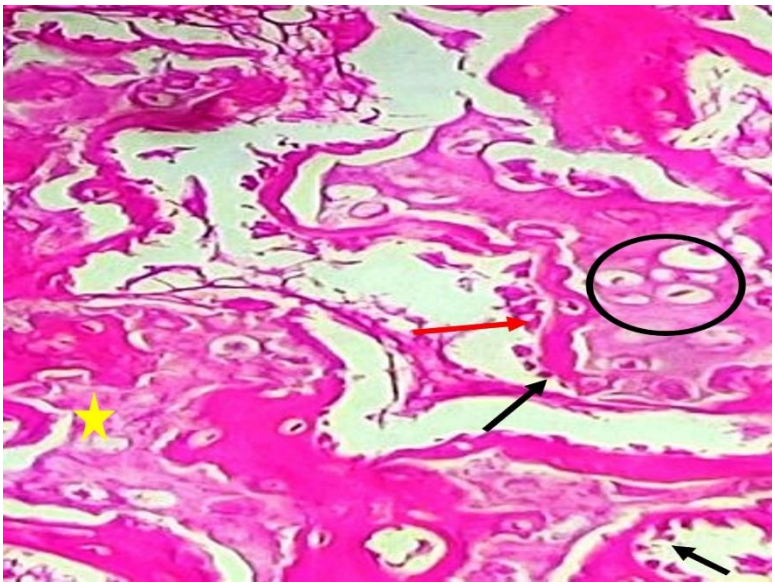

Figure 4.17 Histopathological findings in control group at 4th week post operation show osteocyte proliferative (black circle) and osteoblast and osteoclast proliferative (black and red arrow), with calcified bone formation (yellow star), H&E, 400X.

While the treated group shows increase thickness of mature bone filling the defect area, which is represented by the existence of haversian system with arrangement of osteocytes around the canal of haversian system, as well as osteo matrix scoring (++) and occupying moderate grade (Figure 4.18). Osteoblast arranged in cords in the regenerated bone which surrounded with fibrovascular tissue, (Figure 4.19), Table (4.1).

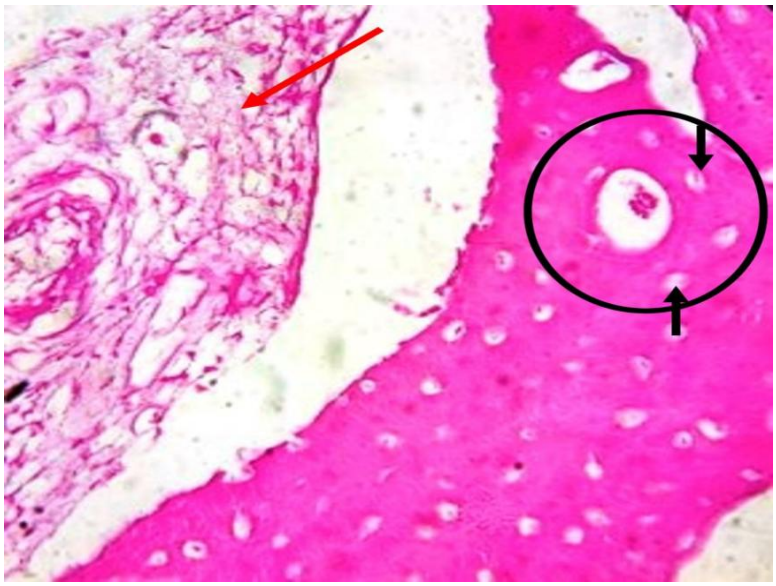

Figure 4.18 Histopathological findings in treated group at 4th week post operation show haversian system (black circle) with osteocytes around the canal (small black arrow), moderate mature osteogenic matrix (red arrow), H&E, 400X.

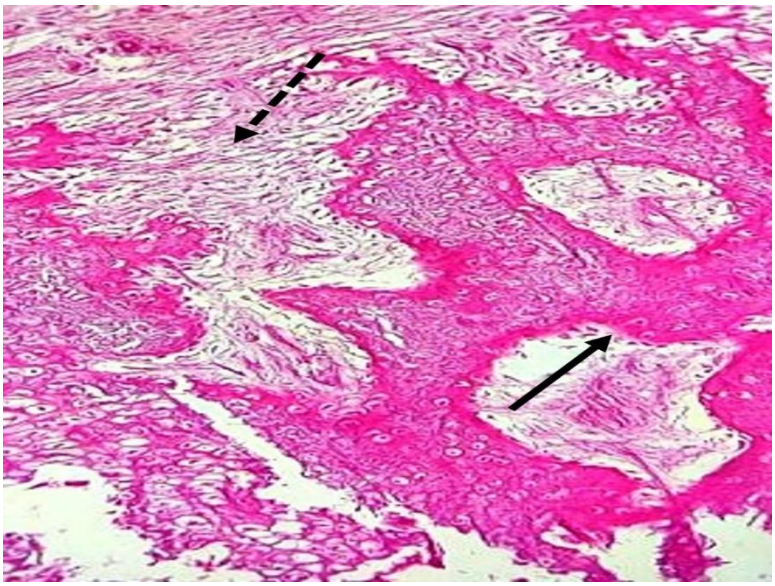

Figure 4.19 Histopathological findings in treated group at 4th week post operation show osteoblast arrangement as cord I (black arrow) with fibrovascular tissue (black- dash arrow), H&E, 100X.

At the 6th week, histological investigation of the distal radial fracture site of the control group showed well developed trabecular bone (Figure 4.20) with newly formed haversian system and osteocyte in their lacuna, lining with osteoblasts and moderate osteon (Figure 4.21) and table (4.1).

Figure 4.20 Histopathological findings in control group at 6th week post operation show well developed trabecular bone (yellow arrow), H&E, 100X.

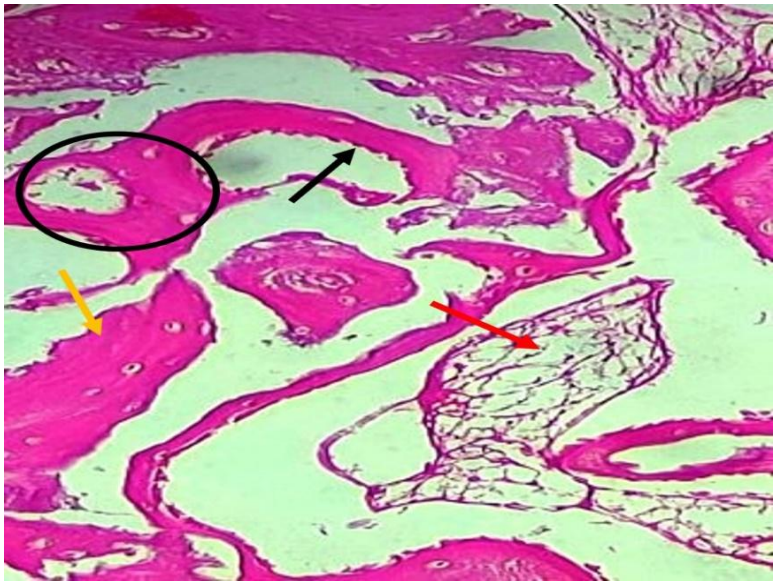

Figure 4.21 Histopathological findings in control group at 6th week post operation show developed trabecular bone (yellow arrow), newly haversian system formation (black circles), cord appearance of osteoblast (black arrow) and moderate osteon tissue (red arrow), H&E, 100X.

While the microscopic examination in biopsy of the operating site of treated group shows thickening of the mature trabecular bone formation around haversian canal, compact lamellar bone formation, mature bone contain osteocyte in their lacuna with sever mature eosinophilic osteoid tissue (well blood vessels, osteogenic connective and adipose tissue) (Figure 4.22), with number of osteoblasts arranged as cord and mild osteoclasts (Figure 4.23).

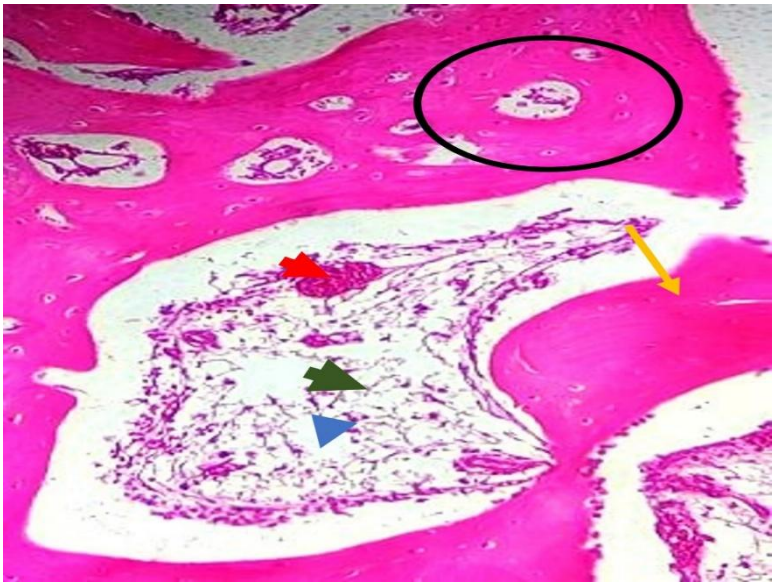

Figure 4.22 Histopathological findings in treated group at 6th week post operation show thickening of mature bone trabeculae and compact lamellar formation (yellow arrow), haversian system (black circle), sever mature eosinophilic osteoid tissue involve blood vessels (red head arrow), adipose tissue (green head arrow) with fibrous connective tissue (blue arrow), H&E, 100X.

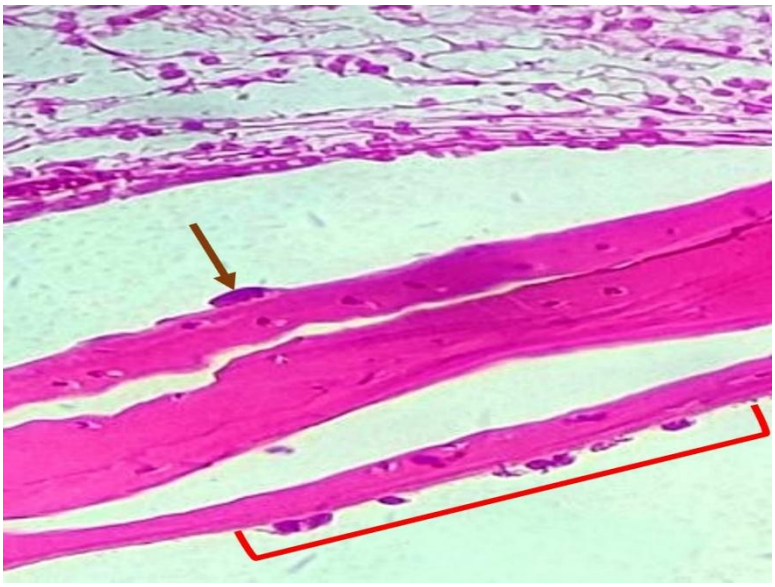

Figure 4.23 Histopathological findings in treated group at 6th week post operation show mild osteoclasts (brown row) and cord like appearance of osteoblasts (red bracket), H&E, 400X.

At the 8th week, histological investigation of the distal radial fracture site of the control group shows regenerated bone (Figure 4.24), well develop and beginning maturation of bone trabeculae with osteon-haversian system (Figure 4.25).

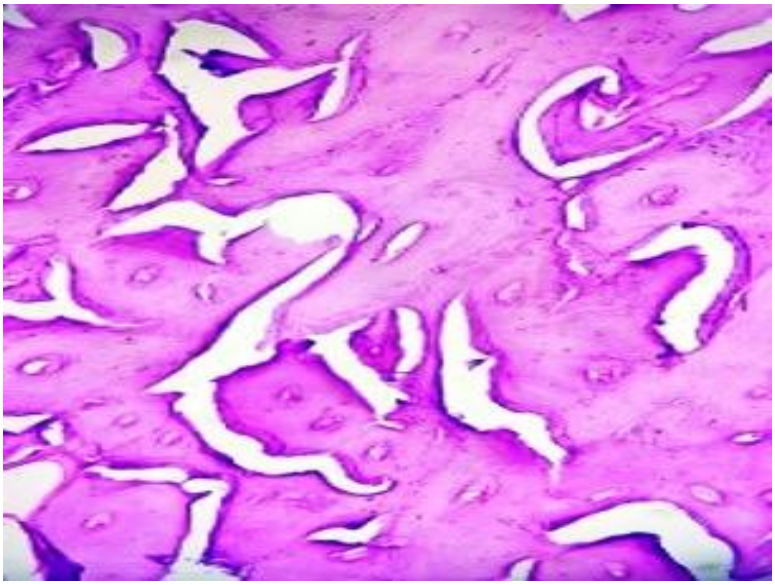

Figure 4.24 Histopathological findings in control group at 8th week post operation show regenerated bone, H&E, 100X.

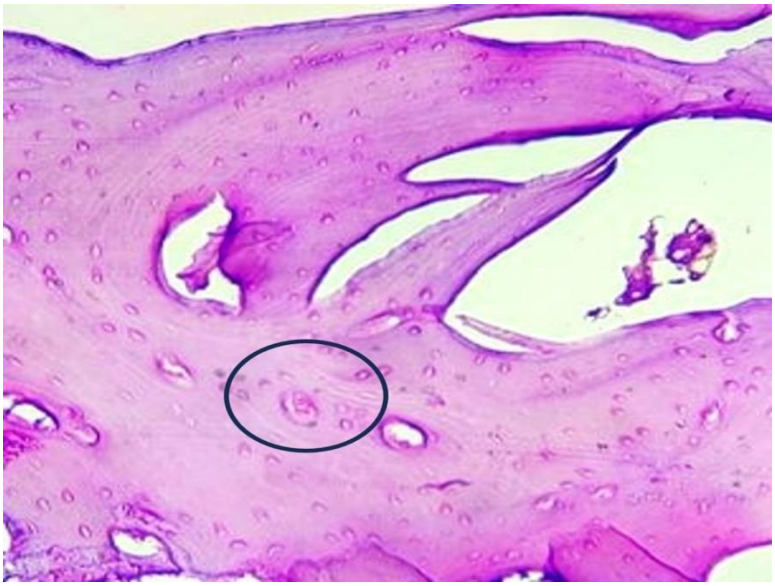

Figure 4.25 Histopathological findings in control group at 8th week post operation show well develop and beginning maturation of bone trabeculae with osteon-haversian system (blue circle), H&E, 400X.

While the microscopic examination in biopsy of the operating site of treated group shows lamina propria-connective tissue, periosteum, periosteum and bone continuity (Figure 4.26), mature osteogenic matrix (Figure 4.27), greater mature bone with osteon-haversian system (Figure 4.28).

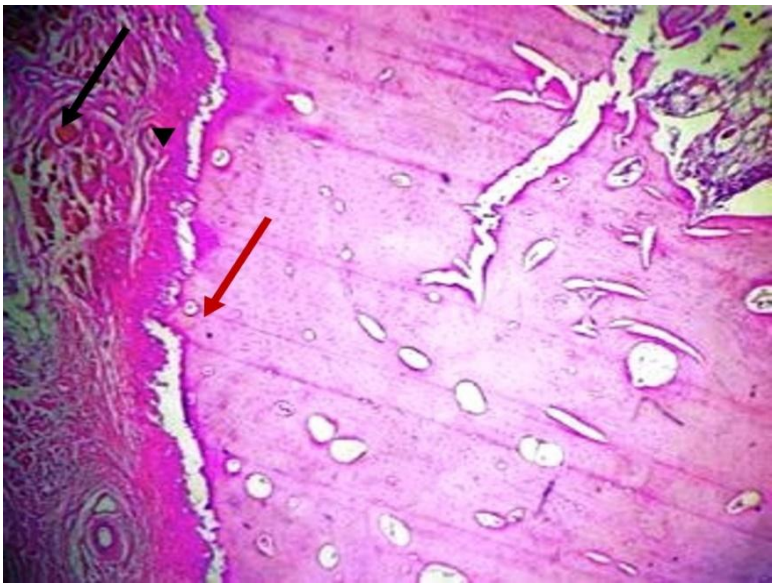

Figure 4.26 Histopathological findings in treated group at 8th week post operation show lamina propria connective tissue (black arrow), periosteum (head black arrow), periosteum and bone continuity (red arrow), H&E, 40X.

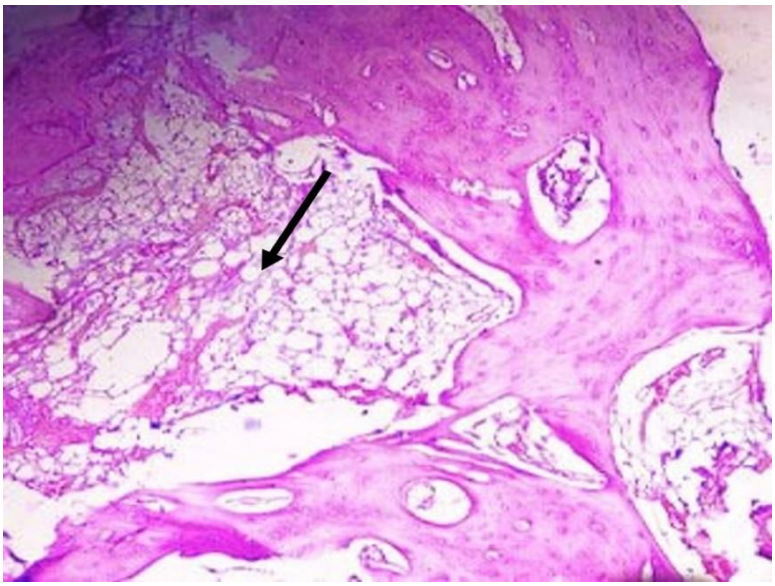

Figure 4.27 Histopathological findings in treated group at 8th week post operation show mature osteogenic matrix (black arrow), H&E, 100X.

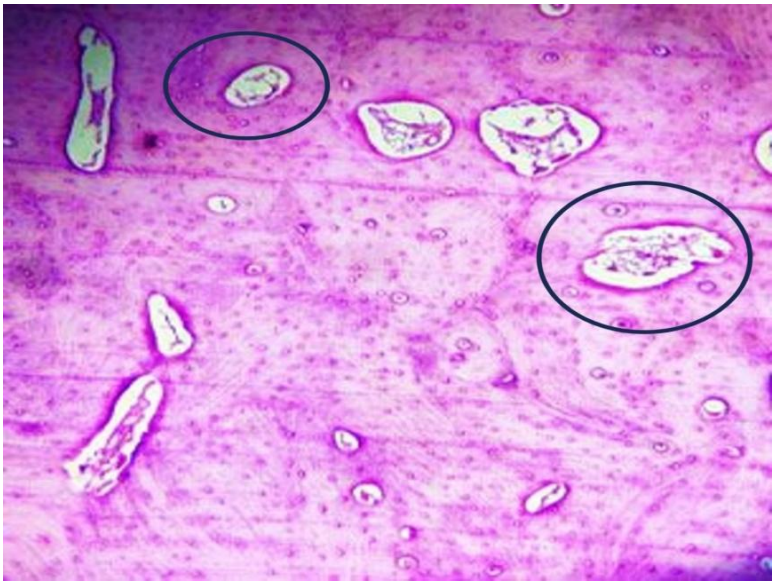

Figure 4.28 Histopathological findings in treated group at 8th week post operation show greater mature bone with osteon-haversian system (blue circle), H&E, 400X.

4.3.1 Histochemical analysis

The below results are further confirm using Masson Trichrome staining which reveal proliferation of chondrocytes indicative cartilaginous callus which stain blue color at score (++ and +++) in both control and treated groups respectively at 2nd week post operation (Figure 4.29) also the histological section shows newly blood vessels formation and old bone with dark blue stain (+++) (Figure 4.30).

At the 4th week post operation in the control group the section analysis reveals irregular bony callus mild (+) blue stain of Masson Trichrome (Figure 4.31), photomicrograph analysis of sections were taken from the fracture site in treated group at the same period post operation reveal mature, thin bone trabeculae and stained with dark / faint blue (Figure 4.32), this results were investigated on regeneration bone from fracture site in dogs in the control group at 6th week post operation (Figure 4.33).

At the 6th week histochemical analysis investigation of the fracture site of the treated group well developed thick trabecular severe blue stain (+++) (Figure 4.34).

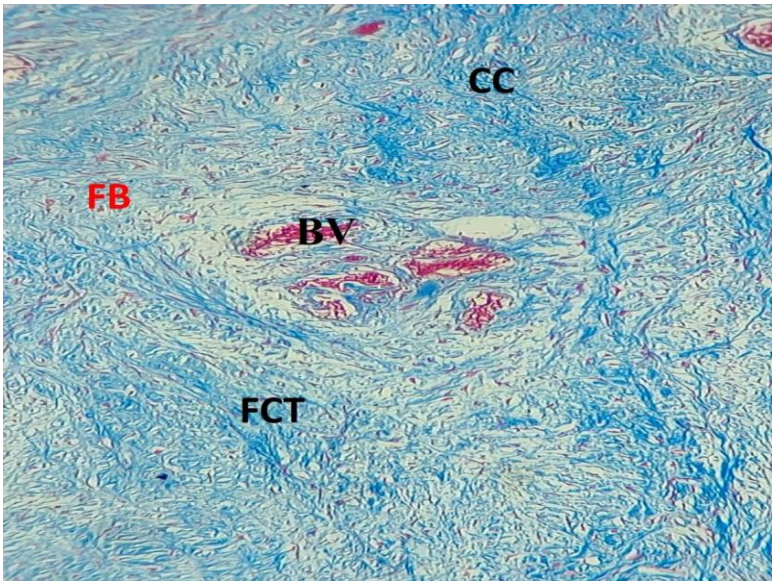

Figure 4.29 Histopathological findings in control group at 2nd week post operation shows cartilaginous callus formation occupies score (++) chondrocyte (CC), fibrous connective tissue (FCT), fibroblast (FB), blood vessels (BV), Masson Trichrom, 100X.

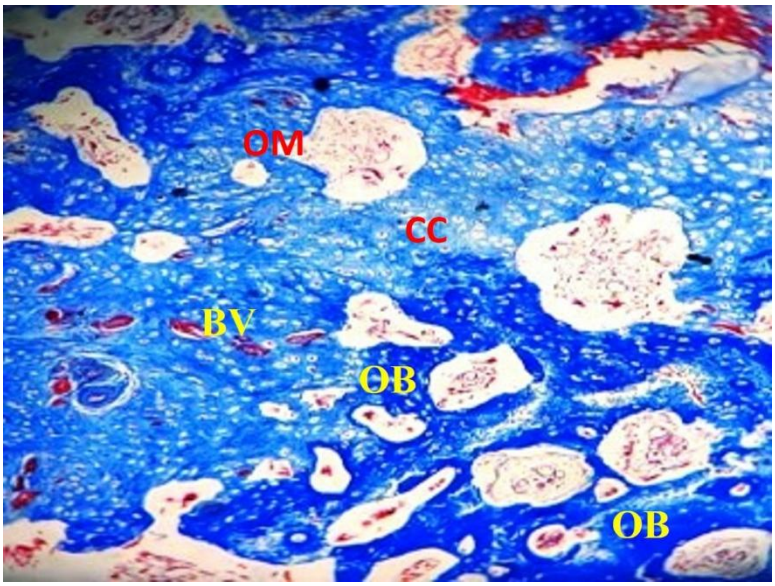

Figure 4.30 Histopathological findings in treated group at the 2nd week post operation shows cartilaginous callus formation occupies score (+++) osteo-matrix (OM), blood vessels (BV), old bone (OB), condrocytes (CC), Masson Trichrom, 100X.

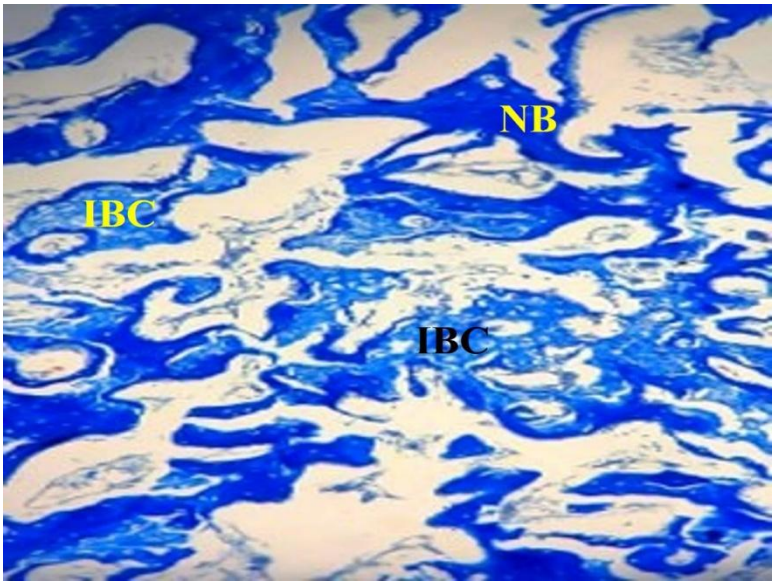

Figure 4.31 Histopathological findings in control group at the 4th week post operation shows irregular bony callus mild (+), newly bone (NB), intra bony callus (IBC), Masson Trichrom, 100X.

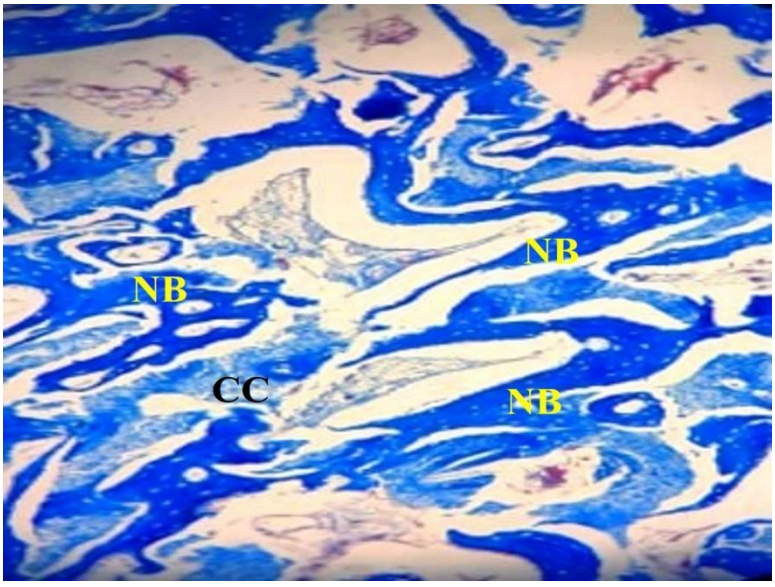

Figure 4.32 Histopathological findings in treated group at 4th week post operatin represents mature thin bone trabeculae dark / faint blue (+++), newly bone (NB), condrocytes (CC), Masson Trichrom, 100X.

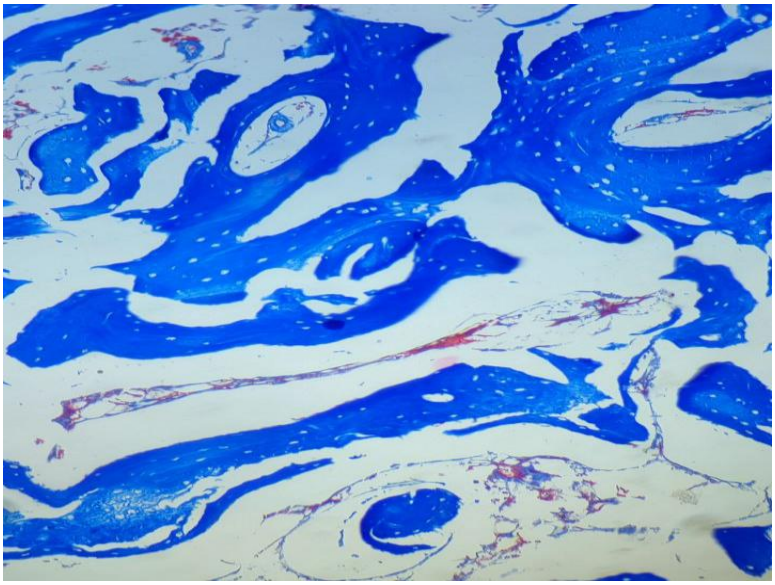

Figure 4.33 Histopathological findings the control group at the 6th week post operation represented regeneration bone, Masson trichrome, 100X**.**

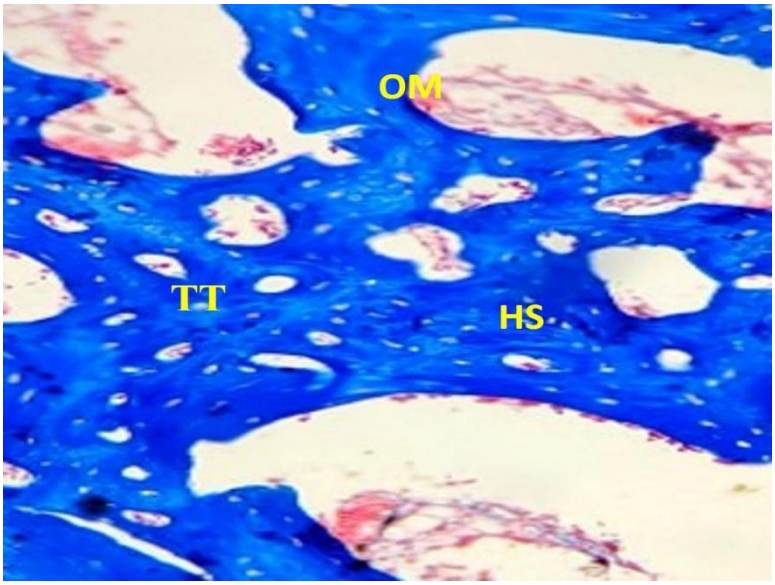

Figure 4.34 Histopathological findings in the treated group at the 6th week post operation represented well developed and thick trabeculae with sever blue stain, thick trabeculae (TT), haversian system (HS), osteomatrix (OM), Masson Trichrom, 400X.

Semi quantitative analysis of Alizarin / Alcian blue for cartilage and bone callus formation were investigated in this study, which reveal apposite correlation between these two structures, at 2nd week the histological criteria of fracture healing occupy grade I (Score +++ for cartilaginous callus and + for bone formation) this criteria is more clearly and intense in treated group (Table 4.2), (Figure 4.35 and 4.36).

The experimental study for period 4th week, reveal improve bone fracture healing in both groups but variable in severity, so the grad / score categories of control group occupy grade II with score (++) for cartilaginous bone like-structure stain with Alcian blue and same score for orange-red (Alizarin stain) for bon structure stain (Table 4.2), (Figure 4.37), while in treated group the photomicrograph analysis reveal that histopathological lesions occupy grade Ⅲ with (+) cartilaginous island stain faint Alcian blue and intense bone trabeculae stained with (+++) orange-red (Table 4.2), (Figure 4.38).

At the 6th week the result of control group occupies grade Ⅲ (Figure 4.39), while in treated group the results occupy grade Ⅳ (Table 4.2), with -ve / non cartilaginous formation and strong intense (++++) of bone trabecular formation (Figure 4.40).

The statistical analysis results showed significant increase ($p \leq 0.05$) in rate number of osteocytes in control group at 6th week post operation that reaches to rate (32.6) cell / field, and the treated group at the 4th week post operation reach the rate (33.8) cell / field in comparison with the other time periods within the same group, and between two groups (Table 4.3), it was noticed also significant superiority of the haversian system in treated group at 2nd and 6th week (3.4, 3.40)

respectively in comparison with the 4th week and also the comparison with the control group (Table 4.3).

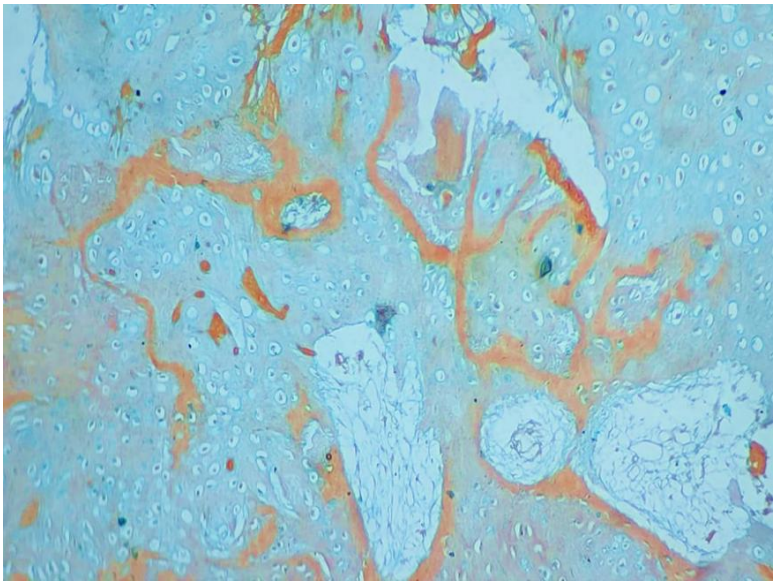

Figure 4.35 Histopathological findings in the control group at the 2th week post operation show cartilaginous callus, Alizarin / Alcian blue, 100X.

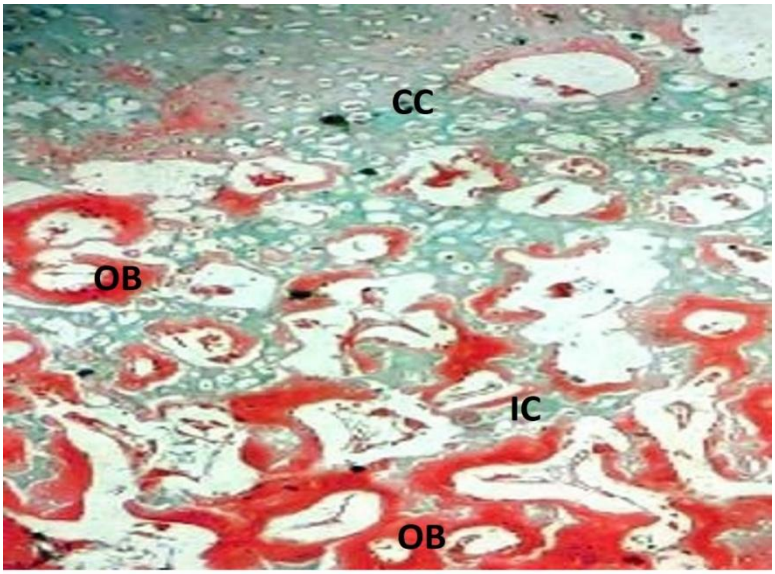

Figure 4.36 Histopathological findings in treated group at 2nd week post fracture show Cartilaginous callus blue stain occupies grade I and score (+++) and orange red stain for bone formation, condrocytes (CC), intra cartilaginous callus (IC), old bone (OB), Alizarin / Alcian blue, 100X.

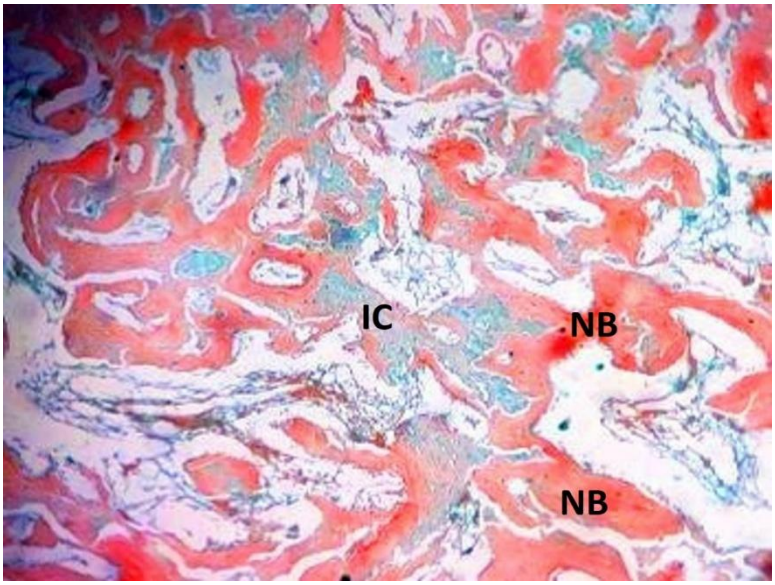

Figure 4.37 Histopathological findings in control group at 4th week post fracture show cartilaginous callus formation occupies grade II score (++), intra cartilagenous (IC), newly bone (NB), Alizarin / Alcian blue, 100X.

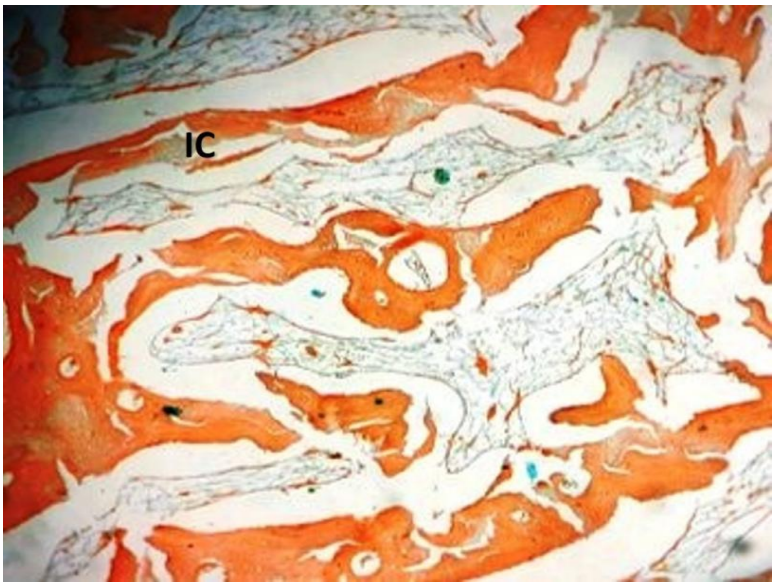

Figure 4.38 Histopathological findings in treated group at the 4th week post fracture show cartilaginous callus stain faint Alcian blue at the grade III and score (+) with orange-red Alizarin stain for bone formation occupy (+++), intracartilagenous (IC), Alizarin / Alcian blue, 100X.

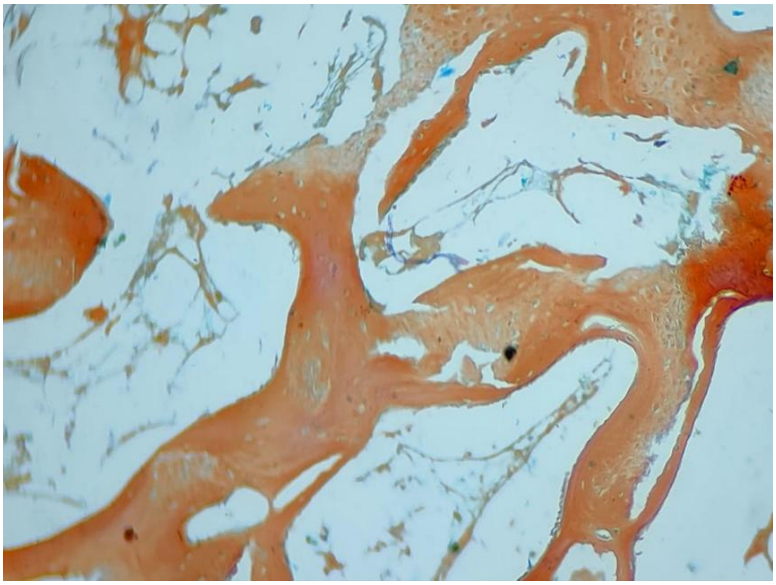

Figure 4.39 Histopathological findings in control group at the 6th week post fracture show cartilagenous island stin faint Alcian blue occupy grade III with score (+) and intense bone trabeculae stained with (+++) orange- red, Alizarine / Alcian blue, 400X.

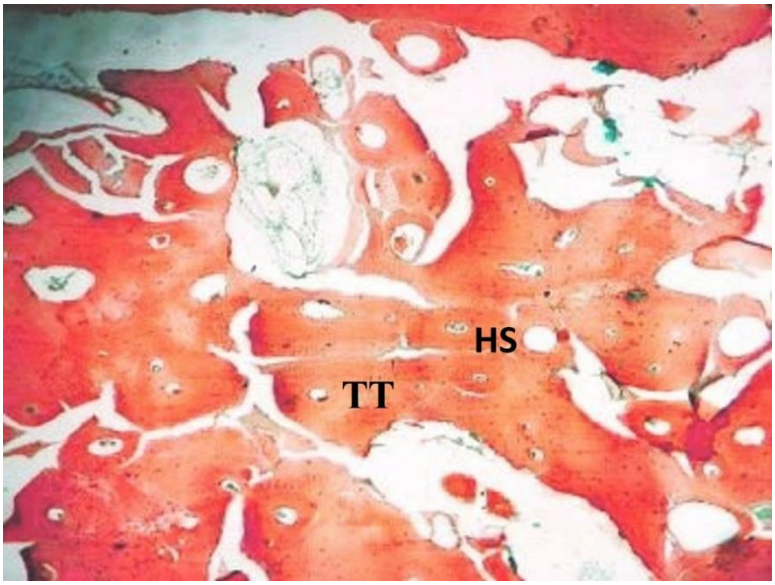

Figure 4.40 Histopathological findings in treated group at the 6th week post fracture represents bone healing criteria occupy grade IV and strong intense (++++) orange-red, thick trabeculae (TT), haversian system (HS), Alizarine / Alcian blue, 400X.

4.3.2 Statistical analysis

Table 2 Score-Grade system and descriptive analysis of histological criteria of fracture bone healing.

Score / Grade Descriptive Analysis				
Fracture / Weeks	**Groups**	**Osteogenic Matrix**	**Osteoclast**	**Trabeculae**
2	**Control**	+ / mild	+++ / sever	irregular, thin trabeculae
	Se-Np	++ / moderate	++ / moderate	regular thin (channels)
4	**Control**	+ / mild	++ / moderate	irregular, thicker trabeculae
	Se-Np	++ / moderate	+ / mild	thicker trabeculae
6	**Control**	++ / moderate	mild	well trabeculae
	Se-Np	+++ /sever	none / mild	thicker trabeculae
8	**Control**	+++ / sever	mild	thicker trabeculae
	Se-Np	+++ / sever	none	thicker trabeculae

Table 3 Semi quantitative analysis of some histological criteria of fracture bone healing (Osteocyte and Haversian system).

Fracture / Weeks	Osteocytes			Haversian Canal	
	Control	Se-Np		Control	Se-Np
2	7.2+0.84 a A	20.2+1.10 b A		1.4+0.12 a A	3.4+0.22 b A
4	13.4+1.52 a B	33.8+1.10 b B		2.2+0.23 a A	7.4+0.22 b B
6	32.6+1.34 a C	26.26+0.89 b C		4.00+0.23 a B	11.40+0.28 b C
8	28.2+0.75 a D	19.7+0.50 b A		10.34+0.15 a C	15.80+0.21 b D

Different small letters mean there is a significant difference between the two groups while the different capital letters indicate a significant difference in the same group at $P \leq 0.05$.

Chapter five

Discussion

5.1 Distal radial fracture in dogs

The distal radial fracture is one of the most common fractures in dogs, and the animals affected with this type of fractures usually suffer from delay or nonunion which is considered one of the challenges that face the animals' owners because of the efforts and expenses of treatment, in some cases the affected animals suffer from pain and lameness for long periods and this is confirmed by many researchers (Harasen, 2003b; Ali, 2013; Watrous and Moens, 2017). Because of the large amount of weight bear of radius bone and little soft tissue overlying the bone with limited blood supply especially in distal third, all these reasons are considered challenges to healing of distal radial fractures and lead to delay or failure of bone union (Harasen, 2003b), and because of the reasons mentioned above we have made up this experimental study by the addition of nano material such as selenium nanoparticles which have osteo inductive action and promotion of fracture healing which are confirmed by researchers (Li *et al*., 2019; Lee *et al*., 2021).

5.2 Clinical examination

Lameness is a key clinical symptom of a distal radial fracture, and it affects every experimental animal. By relied on the grades assessment of dog's gait investigated superiority of the treated group which are faster restoration to semi normal gait at the last stages of study which represented by sound at the walk, but weight shifting and mild lameness noted at trot this agrees with (Watrous and Moens, 2017; Thanoon *et al*.,

2019; Thanoon, 2019) who said that the external fixation can lead to complications as lameness especially in distal radial fracture. It should be noted that the external coaptation by fiber glass cast tape lead to diminished some signs of lameness due to limitation movement of elbow joint and carpal joint, in treated group the lameness becomes less noticeable the superiority of treated group in restoration of semi normal gait post operation that may be due to the effect of Se-NPs which has anti-inflammatory effect this agree with (Lee *et al*., 2021; Karthik *et al*., 2024) who said that Se has anti-inflammatory function. The most important factor that promotes the healing of distal radial fracture is the limitation of movement and prevention of jumping conducted in this experimental study by the caging of the animals in separated cages to decrease the movement and prevent jumping.

5.3 Radiographical examinations

At the 2nd week post operation, the radio-graphical results showed that the fracture line is clear in all experimental animals but there are advanced healing signs such as clear periosteal reaction around the fracture site in treated group in comparison with the control group that shows noticeable fracture line with only small amount of periosteal reaction. This may be due to the addition of Se-NPs on the fracture line in treated group. This agrees with (Zeng *et al*., 2013; Ouyang *et al*., 2023; Yang *et al*., 2024a), who said that Se-NPs enhance the immune response and modulation by activation cytokines which attract the immune cells and trigger migration of cells to the fracture site and platelets continue to aggregate and new blood vessels (angiogenesis) begin to form (Dimitriou *et al.,* 2005). Antioxidant activity that protects the cell from oxidative

stress, also has anti-inflammatory action which interprets why the control group has a little periosteal reaction.

At the 4th week post operation the radio-graphical results shows an increase in periosteal reaction with bridging callus formation that begins to connect both fracture segments in comparison with the control group that shows an increase in periosteal reaction with limited bridging callus formation less than in treated group, this agrees with (Li *et al*., 2019) who said that Se-NPs promotes BMSCS differentiation to osteoblast that secrete collagen-proteoglycan (osteoid) matrix which promotes calcium binding and, consequently, calcification. Bony "spicules," or needle-like bone structures, are created during calcification and extend from the ossification center. The periosteum, which is made of condensed mesenchymal stem cells (MSCs) surrounding the spicules and also enhance osteoblastic proliferation and promote migration BMSCs and improved callus formation (Brannigan and Griffin, 2016).

At the 6th week post operation, the radio-graphical results show a superiority of callus formation in the treated group filling all the fracture line and connecting both fracture segments, rather than in control group the fracture line does not fil completely and still appears. That may be due to the effect of Se-NPs in treated group which stimulated the growth factors, this agrees with (Li *et al*., 2019) who said that Se-NPs can be a promising expression of bone morphogenetic protein (BMP-2) and acceleration of fracture healing, also Se plays an important role in alkaline phosphate (ALP) activation and the expression and inhibition of osteo clasto-genesis and by antioxidant action Se-NPs can promote bone mineral density (Jiménez-Ortega *et al*., 2023; Yang *et al*., 2024b).

At the 8th week post operation the radio-graphical results in treated group showed decrease in the callus size and the bone begins to preserve the normal size and shape which appeared semi normal, rather than in control group which shows radio-opacity with large size of callus around the fracture line, this may be due to effect of Se-NPs in treated group that enhance differentiation of BMSCS to osteoblast, proliferation of osteoblast and migration to the fracture site with the activity of antioxidant and anti-inflammatory action, with activation of growth factors and acceleration of bone healing to reach the normal size and shape confirmed by (Li *et al*., 2019; Kim *et al*., 2021; Zhou *et al*., 2023) who said that Se enhances differentiation of BMSCS to osteoblast and promises bone morphogenetic protein with antioxidant action and accelerate fracture healing and callus formation.

5.4 Histopathological examination

Fracture healing is a major and persistent problem in orthopedic surgery in farm animals, fractures usually occur as a result of traffic accidents and falls from heights, in addition to the inability to restrict the movement of animals for a long period of time. Therefore, there have been many studies are aquired to find medical treatments that accelerate the process of healing of fractures and reduce complications such as necrosis of blood vessels, inflammation, and non-union of bones (Aydin *et al*., 2014).

Selenium nanoparticles have a strong therapeutic effect against cancer cells, pathological microorganisms and neurological diseases and are a preventive and protective factor for the liver against many diseases (Krishnan *et al*., 2019; Yuan *et al*., 2020)

As the microscopic examination of the tissue sections taken from the animals of the treated group at the end of the 2nd week post operation shows the formation of thin cartilaginous bone canals with the formation of dense bone trabeculae at the edge of the fracture compared to the control group. The microscopic examination shows the formation of thin irregular bony trabeculae with the presence of fibrocartilaginous calluses.

This is shown by the semi-quantitative analysis of the staining degree (+++) for Masson's Trichrome stain in the treated group, this is a vital indicator of increased proliferation of chondrocytes which play a role in the healing process. This result is consistent with what researcher Zou *et al* (2024) indicate about the effective role of Se-NPs in stimulating infiltration and proliferation of cells which play an effective role in bone healing and osteo activation, and researcher Hosnedlova *et al* (2018) mention the role of selenium in regulating and differentiation of bone cells.

The results of the statistical analysis shows the significant superiority of osteocytes and also the significant superiority of the haversian system in the treated group compared to the control group, with moderate proliferation of osteoblasts which play a role in the formation of bone matrix at the 4th week, and a decrease in the proliferation of osteoclasts and the formation of bone lamellae at the 6th week post treatment compared to the control group, and this is observed when conducting the semi-quantitative analysis Alizarin/Alcian Blue stained tissue sections at the 4th week post-fracture it is shown that the histopathological alterations in the tissue sections obtained from the treated group and indicative of the formation of cartilaginous tissue are at the grade III and score (+) for the Alcian Blue stain and the appearance of

the bone trabeculae in red-orange color occupy sever grade at score (+++).

When the treatment continued until the 6th and 8th week, it was noted that the tissue sections were not stained with Alcian Blue stain while severe intense score (++++) for the Alizarin stain, as is shown in histological image (4.41), these results are consistent with the results of the study by (Fatima *et al*., 2021), and they indicate that low concentrations of Se-NPs particles have the ability to differentiate osteoblasts from human mesenchymal stem cells (HMSCs) and maturation of cells, which has a role in the process of formation osteogenic matrix and mineralization. Therefore, the results of this study are consistent with the results of the study of the researcher Lee *et al* (2021), whom indicate the stimulating role of Se-NPs for the formation and maturation of osteogenic matrix in the cellular medium MC3T3-E1 cells post 3 and 7 days from Se-NPs injected in the cellular medium.

The results of previous studies have indicated that osteoblasts-osteoclasts communication leads to regulation in the process of healing and bone formation, this communication may be through direct connection between cells or the production and secretion of proteins or cytokines, as osteoblasts secrete molecules (M-CSF, RANKL/ OPG) some of which may have a stimulating or inhibiting role for osteoclasts (Chen *et al*., 2018; Kim *et al*., 2020).

Selenium effects on the manufacture of parathyroid hormone related protein (PTHrP) have a role in the maturation of cartilage cells during the endochondral-ossification process (Ren *et al*., 2007; Yang *et al*., 2016), in addition to what the results of previous studies indicate in that the topical use of selenium has an important role in bone formation

and its high affinity property to calcium phosphate, which is like cement for bone formation (Liu *et al*., 2012; Vaquette *et al*., 2020; Xiao *et al*., 2020).

Therefore, the histopathological dynamics of radius bone healing in animals of the treated group in this study is faster when compared with the control group and these results are consistent with the results of the study of researcher (Al-Heeti *et al*., 2024) whom indicate the role of Se-NPs for titanium implants in the growth, mineralization and maturation of bone in rabbits within six weeks.

There is another metabolic pathway for selenoprotein as an antioxidant. It is known that the early stages of fracture healing lead to the release of reactive oxygen species (ROS), which are sequelae of inflammatory cell infiltration and the release of chemical mediators and cytokines, in addition to injury of blood vessels and tissues, which leads to cell death. These factors may affect the process of fracture healing (Kubo *et al*., 2019; Cotor *et al*., 2023), in addition to the excessive activity of osteoclasts, which is considered as a factor for increasing oxidative stress (OS), therefore, Se-NPs activates selenium proteins especially Lentinan-Se (LNT-Se), which shows cellular aggregation and accumulation and metabolic metabolism of the protein selenocysteine (SeCys 2), which is an important metabolic compound and an effective center for treating oxidative stress and removing free radicals. It is also an inhibitor of the NF-Kb-RANKL axis, which is important for the process of formation. and differentiation of osteoclasts (osteoclast genesis) (Zeng *et al*., 2013; Zou *et al*., 2024), in addition to role of seleno-proteins to stimulating Se dependent antioxidant enzymes such as glutathione (GPx) (Zhou *et al*., 2023).

Conclusions

1- Local application of selenium nanoparticles on the fracture line has a good effect for acceleration the healing process of the distal radial fracture.

2- Fiber glass cast tape proved its efficiency in fixation of distal radial fracture.

Recommendations

1- Using of Se-NPs in combination with biomaterials.

2- Make up micro computed tomographic examination to estimate the degree of ossification at the fracture site.

3- Future studies should be focus on optimizing of Se-NP dosage in dogs.

4- Comparison of Se-NPs with the other nanoparticles such as Ag or ZnO nanoparticles.

5- Administration of Se-NPs orally or parenteral in addition to its local use.

6- Molecular studies are required for further investigations.

References

Albrektsson, T.; and Johansson, C. (2001). Osteoinduction, osteoconduction and osseointegration. European spine journal, 10(2): S96-S101.

Alheeti, O. A.; and Fatalla, A. A. (2021). Evaluation of the anti-bacterial effect of selenium nanoparticles in peri-implantitis patients. J Res Med Dent Sci, 9(12): 96-101.

Alheeti, O. A.; Jani, G. H., & Qustanteen, F. R. (2024). The Effects of Selenium Nanoparticles on the Osseointegration of a Titanium Implant in Rabbits: A Histomorphometric Investigation. Dentistry 3000, 12(2).

Allison, D. C.; Lindberg, A. W.; Samimi, B.; Mirzayan, R.; & Menendez, L. R. (2011). A comparison of mineral bone graft substitutes for bone defects. Oncology & Hematology Review (US), 7(1): 38.

Ali, L. B. (2013). Incidence, occurrence, classification and outcome of small animal fractures: a retrospective study (2005-2010). International Journal of Animal and Veterinary Sciences., 7(3): 191-196.

Astur, D. C.; Zanatta, F.; Arliani, G. G.; Moraes, E. R.; Pochini, A. D. C.; and Ejnisman, B. (2016). Stress fractures: definition, diagnosis and treatment. Revista brasileira de ortopedia, 51: 03-10.

Aydin, A.; Halici, Z.; Akoz, A.; Karaman, A.; Ferah, I.; Bayir, Y.; and Kovaci, H. (2014). Treatment with α-lipoic acid enhances the bone healing after femoral fracture model of rats. Naunyn-Schmiedeberg's archives of pharmacology, 387: 1025-1036.

Bahadar, H.; Maqbool, F.; Niaz, K.; and Abdollahi, M. (2016). Toxicity of nanoparticles and an overview of current experimental models. Iranian biomedical journal, 20(1): 1.

Belu, C.; Dumitrescu, I.; Georgescu, B.; ROȘU, P. M.; ȘEICARU, A.; RAITA, Ș. M. and Predoi, G. (2021). Morphological study of the thoracic limb joints in dogs. Scientific Works. Series C, Veterinary Medicine, 67(2).

Bennour, E.M.; Abushhiwa, M.A.; Ben Ali. L.; Sawesi, O.K.; Marzok, M.A.; Abuargob, O.M.; Tmumen, S.K.; Abdelhadi, J.A.; Abushima, M.M.; Benothman, M.E.; Said, E.M.; and ElKhodery, S.A. (2014). A Retrospective Study on Appendicular Fractures in Dogs and Cats in Tripoli ‐ Libya. J. Vet. Adv., 4(3): 425-431.

Bernstein, HS. (2011). Tissue engineering in regenerative medicine. In: Boyd, NR., Boyd, RL., Simon, GP., Nisbet, DR., Eds. Synthetic multi-level matrices for bone regeneration. Springer. Pp. 99-122.

Bindhu, M. R.; Umadevi, M.; Micheal, M. K.; Arasu, M. V.; and Al-Dhabi, N. A. (2016). Structural, morphological and optical properties of MgO nanoparticles for antibacterial applications. Materials Letters, 166: 19-22.

Blumer, M. J. (2021). Bone tissue and histological and molecular events during development of the long bones. Annals of Anatomy-Anatomischer Anzeiger, 235, 151704.

Borch, W. R.; Aguilera, N. S.; Brissette, M. D.; O'Malley, D. P. and Auerbach, A. (2019). Practical applications in immunohistochemistry: an immunophenotypic approach to the spleen. Archives of pathology & laboratory medicine, 143(9): 1093-1105.

Brannigan, K. and Griffin, M. (2016). Suppl-3, M2: An Update into the Application of Nanotechnology in Bone Healing. The Open Orthopaedics Journal, 10: 808.

Cao, J. J.; Gregoire, B. R.; and Zeng, H. (2012). Selenium deficiency decreases antioxidative capacity and is detrimental to bone microarchitecture in mice. The Journal of nutrition, 142(8): 1526-1531.

Carr, B. J. and Dycus, D. L. (2016). Canine gait analysis. Recovery & Rehab, 6(2): 93-100.

Cavalu, S.; Antoniac, I. V.; Fritea, L.; Mates, I. M.; Milea, C.; Laslo, V.; and Mohan, A. (2018). Surface modifications of the titanium mesh

for cranioplasty using selenium nanoparticles coating. Journal of Adhesion Science and Technology, 32(22): 2509-2522.

Chen, X.; Wang, Z.; Duan, N.; Zhu, G.; Schwarz, E. M.; and Xie, C. (2018). Osteoblast–osteoclast interactions. Connective tissue research, 59(2): 99-107.

Cotor, D. C.; Dragosloveanu, S.; Ionescu, A.; Zagrai, G. and Damian, A. (2023). Effect of Sodium selenite administration on the process of tendon healing in Wistar male rats. Experimental and Therapeutic Medicine, 25(4): 1-6.

Cottrell, J. A.; Turner, J. C.; Arinzeh, T. L.; and O'Connor, J. P. (2016). The biology of bone and ligament healing. Foot and ankle clinics, 21(4): 739-761.

Decamp, C.E.; Johnston, S.A.; Déjardin, L.M. and Schaefer S.L. (2016). Bone grafting. In Piermattei and Flo's handbook of small animal orthopedics and fracture repair. Eds., Decamp, C.E., Johnston, S.A., Déjardin, L.M. and Schaefer, S.L., St. Louis, MO: Elsevier, Pp: 153–162.

Della Nina, M.I.; Schmaedecke, A.; Romano, L. and Ferrigno, C.R.A. (2007). Comparação de osteossíntese com placa e osteossíntese com placa associada a enxerto de proteína morfogenética óssea em fratura bilateral distal de rádio e ulna em cão - relato de caso. Braz. J. Vet. Res. Anim. Sci., 44: 297-303.

Dimitriou, R.; Tsiridis, E. and Giannoudis, P. V. (2005). Current concepts of molecular aspects of bone healing. Injury, 36(12): 1392-1404.

Dowson, C.; Smith, J.; and Brown, T. (2022). Understanding Bone Fractures: A Comprehensive Review. Journal of Orthopedic Research, 45(3): 234-245.

Dutta, PK. and Dutta, J. (2013). Multifaceted development and application of biopolymers for biology, biomedicine and nanotechnology. In: Bhowmick, A.; Banerjee, S.; Kumar, R.; Kundu, PP.; Eds. Hydroxyapatite-packed chitosan-PMMA

nanocomposite: A promising material for construction of synthetic bone. Springer. Pp: 135- 67.

El-Sayed, H.; Morad, M. Y.; Sonbol, H.; Hammam, O. A.; Abd El-Hameed, R. M.; Ellethy, R. A.; and Hamada, M. A. (2023). Myco-Synthesized Selenium Nanoparticles as Wound Healing and Antibacterial Agent: An In Vitro and In Vivo Investigation. Microorganisms, 11(9): 2341.

Evans, H.E. and Alexander, L. (2017). Guide to the Dissection of the Dog (8th ed.). St. Louis, Missouri: Elsevier.

Fatima, S.; Alfrayh, R.; Alrashed, M.; Alsobaie, S.; Ahmad, R. and Mahmood, A. (2021). Selenium nanoparticles by moderating oxidative stress promote differentiation of mesenchymal stem cells to osteoblasts. International Journal of Nanomedicine, 331-343

Geris, L.; Gerisch, A.; Vander Sloten, J.; Weiner, R. and Van Oosterwyck, H. (2008). Angiogenesis in bone fracture healing: a bioregulatory model. Journal of theoretical biology, 251(1). Pp: 137-158.

Giganti, M.G.; Tresoldi, I.; Masuelli, L.; Modesti, A.; Grosso, G.; Liuni, F.M.; Celi, M.; Rao, C.; Gasbarra, E.; Bei, R. and Tarantino, U. (2014). Fracture healing: From basic science to role of nutrition. Frontier. Biosci. J., 19: 1162-1175.

Goldhahn, J.; Féron, J. M.; Kanis, J.; Papapoulos, S.; Reginster, J. Y.; Rizzoli, R. and Boonen, S. (2012). Implications for fracture healing of current and new osteoporosis treatments: an ESCEO consensus paper. Calcified tissue international, 90(5): 343-353.

Gragossian, A. and Varacallo M. (2020). StatPearls [Internet] StatPearls Publishing; Treasure Island (FL): Radial nerve injury 2020.

Gunti, L.; Dass, R. S. and Kalagatur, N. K. (2019). Phytofabrication of selenium nanoparticles from Emblica officinalis fruit extract and exploring its biopotential applications: antioxidant, antimicrobial, and biocompatibility. Frontiers in microbiology, 10, 931.

Harasen, G. (2003a). Common long bone fracture in small animal practice - Part 2. Can. Vet. J., 44(6): 503-504.

Harasen, G. (2003b). External coaptation of distal radius and ulna fractures. Can. Vet. J., 44(12): 1010-1011.

Hernandez-Gil, I. F. T.; Gracia, M. A.; del Canto Pingarrón, M.; and Jerez, L. B. (2006). Physiological bases of bone regeneration I. Histology and physiology of bone tissue. Med Oral, 11(1): 47-51.

Hosnedlova, B.; Kepinska, M.; Skalickova, S.; Fernandez, C.; Ruttkay-Nedecky, B.; Peng, Q. and Kizek, R. (2018). Nano-selenium and its nanomedicine applications: a critical review. International journal of nanomedicine, 2107-2128.

Huang, B.; Wang, W.; Li, Q.; Wang, Z.; Yan, B.; Zhang, Z. and Bai, X. (2016). Osteoblasts secrete Cxcl9 to regulate angiogenesis in bone. Nature communications, 7(1): 13885.

James, R.; Deng, M.; Laurencin, CT. and Kumbar, SG. (2011). Nanocomposites and bone regeneration. Front Mater Sci. 5(4).

Jiménez-Ortega, R. F.; Aparicio-Bautista, D. I.; Becerra-Cervera, A.; López-Montoya, P.; León-Reyes, G.; Flores-Morales, J. and Velázquez-Cruz, R. (2023). Association Study between Antioxidant Nutrient Intake and Low Bone Mineral Density with Oxidative Stress-Single Nucleotide Variants: GPX1 (rs1050450 and rs17650792), SOD2 (rs4880) and CAT (rs769217) in Mexican Women. Antioxidants, 12(12): 2089.

Kang, D.; Lee, J.; Wu, C.; Guo, X.; Lee, B. J.;Chun, J. S. and Kim, J. H. (2020). The role of selenium metabolism and selenoproteins in cartilage homeostasis and arthropathies. Experimental & molecular medicine, 52(8): 1198-1208.

Kargozar, S. and Mozafari, M. (2018). Nanotechnology and Nanomedicine: Start small, think big. Mater. Today Proceed., 5(7): 15492-15500.

Karthik, K. K.; Cheriyan, B. V.; Rajeshkumar, S. and Gopalakrishnan, M. (2024). A review on selenium nanoparticles and their biomedical applications. Biomedical Technology, 6: 61-74.

Kellam, J.F.; Meinberg, E.G.; Agel,J.; Karam, M.D.; and Roberts, C.S. (2018). Introduction: Fracture and Dislocation Classification Compendium−2018 International Comprehensive Classification of Fractures and Dislocations Committee. J. Orthopa. Trau., 32(1): S1-S10.

Khurana, A.; Tekula, S.; Saifi, M. A.; Venkatesh, P. and Godugu, C. (2019). Therapeutic applications of selenium nanoparticles. Biomedicine & Pharmacotherapy, 111: 802-812.

Kieliszek, M. and Błażejak, S. (2016). Current knowledge on the importance of selenium in food for living organisms: a review. Molecules, 21(5): 609.

Kim, H.; Lee, K.; Kim, J. M.; Kim, M. Y.; Kim, J. R.; Lee, H. W. and Jeong, D. (2021). Selenoprotein W ensures physiological bone remodeling by preventing hyperactivity of osteoclasts. Nature communications, 12(1): 2258.

Kim, J. M.; Lin, C.; Stavre, Z.; Greenblatt, M. B. and Shim, J. H. (2020). Osteoblast-osteoclast communication and bone homeostasis. Cells, 9(9): 2073

Kim, T. H. and Kim, H. Y. (2024). Comparison of different pinning techniques for 3D-printed radius with Salter-Harris type I fracture. The Thai Journal of Veterinary Medicine., 53(1): 15-22.

Kini, U. and Nandeesh, B. N. (2012). Physiology of bone formation, remodeling, and metabolism. Radionuclide and hybrid bone imaging, 29-57.

Kondaparthi, P.; Flora, S. J. S. and Naqvi, S. (2019). Selenium nanoparticles: An insight on its Pro-oxidant and antioxidant properties. Front. Nanosci. Nanotechnol, 6(1): 5.

Krishnan, V.; Loganathan, C. and Thayumanavan, P. (2019). Green synthesized selenium nanoparticles using Spermacoce hispida as carrier of s-allyl glutathione: to accomplish hepatoprotective and nephroprotective activity against acetaminophen toxicity. Artificial cells, nanomedicine, and biotechnology, 47(1): 56-63.

Kubo, Y.; Wruck, C. J.; Fragoulis, A.; Drescher, W.; Pape, H. C.; Lichte, P. and Jahr, H. (2019). Role of Nrf2 in fracture healing: clinical aspects of oxidative stress. Calcified tissue international, 105(4): 341-352.

Lara, H. H.; Guisbiers, G.; Mendoza, J.; Mimun, L. C.; Vincent, B. A.; Lopez-Ribot, J. L. and Nash, K. L. (2018). Synergistic antifungal effect of chitosan-stabilized selenium nanoparticles synthesized by pulsed laser ablation in liquids against Candida albicans biofilms. International journal of nanomedicine, 2697-2708.

Lastayo, P. C.; Winters, K. M. and Hardy, M. (2003). Fracture healing: bone healing, fracture management, and current concepts related to the hand. Journal of Hand Therapy, 16(2): 81-93.

Latef, T. J.; Bilal, M.; Vetter, M.; Iwanaga, J.; Oskouian, R. J.; and Tubbs, R. S. (2018). Injury of the radial nerve in the arm: a review. Cureus, 10(2).

Lauzon, M. A.; Bergeron, É.; Marcos, B. and Faucheux, N. (2012). Bone repair: new developments in growth factor delivery systems and their mathematical modeling. Journal of controlled release, 162(3): 502-520.

Lean, J. M.; Jagger, C. J.; Kirstein, B.; Fuller, K. and Chambers, T. J. (2005). Hydrogen peroxide is essential for estrogen-deficiency bone loss and osteoclast formation. Endocrinology, 146(2): 728-735.

Lee, S. C.; Lee, N. H.; Patel, K. D.; Jang, T. S.; Knowles, J. C.; Kim, H. W.; and Lee, J. H. (2021). The effect of selenium nanoparticles on the osteogenic differentiation of MC3T3-E1 cells. Nanomaterials, 11(2): 557.

Levine, J.M.; Levine, G.J.; Hoffman, A.G.; Mez, J.; and Bratton, G.R. (2007). Comparative Anatomy of the Horse, Ox, and Dog: The Vertebral Column and Peripheral Nerves. Compendium Equine, 2(5): 279-292.

Li, C.; Wang, Q.; Gu, X.; Kang, Y.; Zhang, Y.; Hu, Y.; and Wang, Q. (2019). Porous Se@ SiO2 nanocomposite promotes migration and osteogenic differentiation of rat bone marrow mesenchymal stem cell to accelerate bone fracture healing in a rat model. International Journal of Nanomedicine, 3845-3860.

Li, H.; Guo, Y.; Chen, X.; Man, Z. and Zhang, X. (2023). Effect of different forms of selenium in osteoporosis rat model induced by retinoic acid. Food Quality and Safety, 7, fyad017.

Libardoni, R.N.; Serafini, G.M.C.; Oliveira, C.; Schimites, P.I.; Chaves, R.O.; Feranti, J.P.S.; Costa, C.A.S.; Amara, A.S.; Raiser, A.G. and Soares, A.V. (2016). Appendicular fractures of traumatic etiology in dogs: 955 cases (2004-2013). Ciência Rural, Santa Maria, 46(3): 542-546.

Liu, H.; Bian, W.; Liu, S. and Huang, K. (2012). Selenium protects bone marrow stromal cells against hydrogen peroxide-induced inhibition of osteoblastic differentiation by suppressing oxidative stress and ERK signaling pathway. Biological trace element research, 150: 441-450.

Liu, X.; Mao, Y.; Huang, S.; Li, W.; Zhang, W.; An, J. and Zhou, P. (2022). Selenium nanoparticles derived from Proteus mirabilis YC801 alleviate oxidative stress and inflammatory response to promote nerve repair in rats with spinal cord injury. Regenerative Biomaterials, 9, rbac042.

Majeed, W.; Zafar, M.; Bhatti, A. and John, P. (2018). Therapeutic potential of selenium nanoparticles. J Nanomed Nanotechnol, 9(1): 1.

Marsell, R. and Einhorn, T. A. (2011). The biology of fracture healing. Injury, 42(6): 551-555.

McCartney, W.; Kiss, K. and Robertson, I. (2010). Treatment of distal radial/ulnar fractures in17 toy breed dogs. Vet. Reco. J., 166(14): 430-432.

Mistry, A. S. and Mikos, A. G. (2005). Tissue engineering strategies for bone regeneration. Regenerative medicine Ii: clinical and preclinical applications, 1-22.

Mohammed, F.; Alkattan, L.; Shareef, A. and Ismail, H. K. (2022). The role of adding hyaluronic acid in the grafting process for the repair of an experimentally induced tibial defect in dogs' model. Iraqi J Vet Sci. 36(3): 555-561.

Mountziaris, P. M. and Mikos, A. G. (2008). Modulation of the inflammatory response for enhanced bone tissue regeneration. Tissue Engineering Part B: Reviews, 14(2): 179-186.

Murugesan, G.; Nagaraj, K.; Sunmathi, D. and Subramani, K. (2019). Methods involved in the synthesis of selenium nanoparticles and their different applications-a review. Eur. J. Biomed, 6(4): 189-194.

Myo, N. Z.; Po, S. P.; Soe, H. Y.; Myint, H. H. and Khaing, K. T. (2016). Comparison on Development of Ossification Centres of Radius and Ulna in Male and Female Dogs by Radiographically. IJNRLS, 3(5): 18-29.

Oryan, A.; Alidadi, S. and Moshiri, A. (2013). Current concerns regarding healing of bone defects. J. Hard Tissue., 2(2): 1-12.

Oryan, A.; Monazzah, S. and Bigham-Sadegh, A. (2015). Bone injury and fracture healing biology. Biomedical and environmental sciences, 28(1): 57-71.

Ouyang, J.; Deng, B.; Zou, B.; Li, Y.; Bu, Q.; Tian, Y. and Tao, W. (2023). Oral hydrogel microbeads-mediated in situ synthesis of selenoproteins for regulating intestinal immunity and microbiota. Journal of the American Chemical Society, 145(22): 12193-12205.

Petrie, A. and Watson, P. (2013). Hypothesis tests, the Chi-squared test: comparing proportions. In: Petrie, A., Watson, P. (Eds.), Statistics for veterinary and animal science 3E, (3rd edition). Wiley Blackwell, USA, Pp: 112-126

Pilitsis, J. G.; Lucas, D. R. and Rengachary, S. R. (2002). Bone healing and spinal fusion. Neurosurgical focus, 13(6): 1- 6

Popovitch, C.; Gibson, T.W. and Sylvestre, A.M. (2019). Radius and Ulna. Fracture Management for the Small Animal Practitioner, 105-117, 245-248.

Quester, K.; Avalos-Borja, M. and Castro-Longoria, E. (2013). Biosynthesis and microscopic study of metallic nanoparticles. Micron, 54: 1-27.

Quintana, M.; Haro-Poniatowski, E.; Morales, J. and Batina, N. (2002). Synthesis of selenium nanoparticles by pulsed laser ablation. Applied surface science, 195(1-4): 175-186.

Rankin, E. B.; Wu, C.; Khatri, R.; Wilson, T. L.; Andersen, R.; Araldi, E. and Giaccia, A. J. (2012). The HIF signaling pathway in osteoblasts directly modulates erythropoiesis through the production of EPO. Cell, 149(1): 63-74.

Ren, F. L.; Guo, X.; Zhang, R. J.; Wang, S. J.; Zuo, H.; Zhang, Z. T. and Su, M. (2007). Effects of selenium and iodine deficiency on bone, cartilage growth plate and chondrocyte differentiation in two generations of rats. Osteoarthritis and Cartilage, 15(10): 1171-1177.

Saeed, M.; Ansari, M. T.; Kaleem, I.; Bajwa, S. Z.; Rehman, A.; Bano, K. and Khan, W. S. (2019). Assessment of antimicrobial features of selenium nanoparticles (SeNPs) using cyclic voltammetric strategy. Journal of Nanoscience and Nanotechnology, 19(11): 7363-7368.

Salian, V. (2021). Special Stains in Histopathology: An Oral Pathology Perspective. J Dental Health Oral Res, 2(3): 1-19.

Schell, H.; Duda, G. N.; Peters, A.; Tsitsilonis, S.; Johnson, K. A. and Schmidt-Bleek, K. (2017). The haematoma and its role in bone healing. Journal of experimental orthopaedics, 4(1): 5.

Schindeler, A.; McDonald, M. M.; Bokko, P. and Little, D. G. (2008, October). Bone remodeling during fracture repair: The cellular picture. In Seminars in cell & developmental biology (19)5: 459-46 Academic Press.

Schmidmaier, G.; Wildemann, B.; Heeger, J.; Gäbelein, T.; Flyvbjerg, A.; Bail, H. J. and Raschke, M. (2002). Improvement of fracture healing by systemic administration of growth hormone and local application of insulin-like growth factor-1 and transforming growth factor-β1. Bone, 31(1): 165-172.

Shapiro, F. (2008). Bone development and its relation to fracture repair. the role of mesenchymal osteoblasts and surface osteoblasts. Eur Cell Mater; 15:53-76.

Sheen, J. R.; Mabrouk, A. and Garla, V. V. (2023). Fracture healing overview. In StatPearls [Internet]. StatPearls Publishing.

Shenoy, R. and Pillai, A. (2017). Biology of fracture healing-an overview. Journal of Thoracic Oncology, 5(2): 283-293.

Silva, I. C.; Maia, C. A. A.; Raymundo, A. C.; Prata, M. N. L.; Romero, T. R. L.; Duarte, I. D. G. and Belo, M. A. A. (2021). Meta-analysis of the Therapeutic use of Dipyrone in dogs: Pharmacological effects and clinical safety. Ars Veterinaria, 37(1): 21-30.

Sim, J.H. and Ahn, D. (2014). Anatomy of the diaphyseal nutrient foramen in the long bones of the pectoral limb of German Shepherds. Korean J. Vet. Res., 54(3): 179-184.

Soyab, T. (2020). Special stains used in histopathological techniques: A brief view. Indian J Forensic Med Toxicol, 14(4): 8632-6.

Sreelatha, A.; Yee, S. S.; Lopez, V. A.; Park, B. C.; Kinch, L. N.; Pilch, S. and Tagliabracci, V. S. (2018). Protein AMPylation by an evolutionarily conserved pseudokinase. Cell, 175(3): 809-821.

Suvarna, K. S.; Layton, C. and Bancroft, J. D. (2018). Bancroft's theory and practice of histological techniques. Elsevier health sciences. Pp: 609.

Thanoon, M.; Eesa, M. J. and Abed, E. R. (2019). Effects of platelets rich fibrin and bone marrow on the healing of distal radial fracture in local dogs: Comparative study. Iraqi Journal of Veterinary Sciences, 33(2): 419-425.

Thanoon, M. (2019). A comparative study of effect of autologous implant of bone marrow and platelets rich fibrin on healing of experimental induced radial fracture in dogs, PhD Dissertation: College of Veterinary Medicine, University of Mosul, in partial fulfillment of the requirements for the degree of Doctor of Philosophy in Veterinary surgery 3rd, April, 2019.Mosul-Iraq

Tozzi, G.; Mori, A.D.; Oliveira, A. and Roldo, M. (2016). Composite Hydrogels for Bone Regeneration. J Materials; 9(267): 1-24.

Tran, P. and Webster, T. J. (2008). Enhanced osteoblast adhesion on nanostructured selenium compacts for anti-cancer orthopedic applications. International journal of nanomedicine, 3(3): 391-396.

Tran, P. A.; O'Brien-Simpson, N.; Palmer, J. A.; Bock, N.; Reynolds, E. C.; Webster, T. J. and O'connor, A. J. (2019). Selenium nanoparticles as anti-infective implant coatings for trauma orthopedics against methicillin-resistant Staphylococcus aureus and epidermidis: in vitro and in vivo assessment. International journal of nanomedicine, 4613-4624.

Tran, P. A. and Webster, T. J. (2011). Selenium nanoparticles inhibit Staphylococcus aureus growth. International journal of nanomedicine, 1553-1558.

Vaquette, C.; Bock, N. and Tran, P. A. (2020). Layered antimicrobial selenium nanoparticle–calcium phosphate coating on 3D printed scaffolds enhanced bone formation in critical size defects. ACS Applied Materials & Interfaces, 12(50): 55638-55648.

Wadhwani, S. A.; Shedbalkar, U. U.; Singh, R.; and Chopade, B. A. (2016). Biogenic selenium nanoparticles: current status and future prospects. Applied microbiology and biotechnology, 100: 2555-2566.

Wang, H. Wei, W.; Zhang, S. Y.; Shen, Y. X.; Yue, L.; Wang, N. P.; and Xu, S. Y. (2005). Melatonin-selenium nanoparticles inhibit oxidative stress and protect against hepatic injury induced by Bacillus Calmette–Guérin/lipopolysaccharide in mice. Journal of pineal research, 39(2): 156-163.

Wang, J.; Liu, Z.; He, X.; Lian, S.; Liang, J.; Yu, D. and Wu, R. (2018). Selenium deficiency induces duodenal villi cell apoptosis via an oxidative stress-induced mitochondrial apoptosis pathway and an inflammatory signaling-induced death receptor pathway. Metallomics, 10(10): 1390-1400.

Wang, Q., Larese-Casanova, P. and Webster, T. J. (2015). Inhibition of various gram-positive and gram-negative bacteria growth on selenium nanoparticle coated paper towels. International Journal of Nanomedicine, 2885-2894.

Wang, Y.; Wan, C.; Deng, L.; Liu, X.; Cao, X.; Gilbert, S. R. and Clemens, T. L. (2007). The hypoxia-inducible factor α pathway couples angiogenesis to osteogenesis during skeletal development. The Journal of clinical investigation, 117(6): 1616-1626.

Watrous, G. K. and Moens, N. M. (2017). Cuttable plate fixation for small breed dogs with radius and ulna fractures: Retrospective study of 31 dogs. The Canadian Veterinary Journal, 58(4): 377-382.

Witmer, D.K.; Marshall, S.T. and Browner, B.D. (2016). "Emergency Care of Musculoskeletal Injuries". In Townsend, C., Beauchamp, R., Evers, M., Mattox, K. (eds.). Sabiston Textbook of Surgery (21th ed.). Elsevier. Pp. 440‑504.

Xiao, D.; Zhang, J.; Zhang, C., Barbieri, D., Yuan, H., Moroni, L. and Feng, G. (2020). The role of calcium phosphate surface structure in osteogenesis and the mechanisms involved. Acta biomaterialia, 106: 22-33

Xiong, Z.; Lin, H.; Li, H.; Zou, B.; Xie, B.; Yu, Y. and Chen, T. (2023). Chiral Selenium Nanotherapeutics Regulates Selenoproteins to Attenuate Glucocorticoid-Induced Osteoporosis. Advanced Functional Materials, 33(17): 2212970.

Yang, L.; Zhao, G. H.; Yu, F. F.; Zhang, R. Q. and Guo, X. (2016). Selenium and iodine levels in subjects with Kashin-Beck disease: a meta-analysis. Biological trace element research, 170: 43-54.

Yang, T.; Lee, S. Y.; Park, K. C.; Park, S. H.; Chung, J. and Lee, S. (2022). The effects of selenium on bone health: from element to therapeutics. Molecules, 27(2): 392.

Yang, Y.; Liu, Y.; Yang, Q. and Liu, T. (2024a). The Application of Selenium Nanoparticles in Immunotherapy. Nano Biomedicine and Engineering, 16(3): 345-356.

Yang, Y.; Yang, H.; Feng, X.; Song, Q.; Cui, J.; Hou, Y. and Pei, Y. (2024b). Selenium-Containing Protein from Selenium-Enriched Spirulina platensis Relieves Osteoporosis by Inhibiting Inflammatory Response, Osteoblast Inactivation, and Osteoclastogenesis. Journal of Food Biochemistry, 2024(1): 3873909.

Yuan, X.; Fu, Z.; Ji, P., Guo, L.; Al-Ghamdy, A. O.; Alkandiri, A. and Kassab, R. B. (2020). Selenium nanoparticles pre-treatment reverse behavioral, oxidative damage, neuronal loss and neurochemical alterations in pentylenetetrazole-induced epileptic seizures in mice. International Journal of Nanomedicine, 6339-6353.

Zachara, B. A., Pawluk, H.; Bloch-Boguslawska, E.; Śliwka, K. M.; Korenkiewicz, J.; Skok, Ź. and Ryć, K. (2001). Tissue level, distribution and total body selenium content in healthy and diseased humans in Poland. Archives of Environmental Health: An International Journal, 56(5): 461-466.

Zeng, H.; Cao, J. J. and Combs Jr, G. F. (2013). Selenium in bone health: roles in antioxidant protection and cell proliferation. Nutrients, 5(1): 97-110.

Zhang, L.; Dong, Z.; Zhang, CL. and Gu, YD. (2016). Surgical Anatomy of the Radial Nerve at the Elbow and in the Forearm: Anatomical Basis for Intraplexus Nerve Transfer to Reconstruct Thumb and Finger Extension in C7 _ T1 Brachial Plexus Palsy. J Reconstr Microsurger; 32(9): 670-674.

Zhang, Z.; Zhang, J. and Xiao, J. (2014). Selenoproteins and selenium status in bone physiology and pathology. Biochimica et Biophysica Acta (BBA)-General Subjects, 1840(11): 3246-3256.

Zhou, Q.; Chen, W.; Gu, C.; Liu, H.; Hu, X.; Deng, L. and Liu, T. (2023). Selenium-modified bone cement promotes osteoporotic bone defect repair in ovariectomized rats by restoring GPx1-mediated mitochondrial antioxidant functions. Regenerative Biomaterials, 10, rbad011.

Zhu, M., Niu, G. and Tang, J. (2019). Elemental Se: fundamentals and its optoelectronic applications. Journal of Materials Chemistry C, 7(8): 2199-2206.

Zou, B.; Xiong, Z.; Yu, Y.; Shi, S.; Li, X. and Chen, T. (2024). Rapid selenoprotein activation by selenium nanoparticles to suppresses osteoclastogenesis and pathological bone loss. Advanced Materials, 24016.

الخلاصة

هدفت هذه الدراسة إلى تقييم دور جسيمات السيلينيوم النانوية في التئام كسر عظم الكعبرة القاصي في الكلاب. تم استخدام أربعة وعشرين كلبًا بالغًا سليمًا سريريًا في الدراسة التجريبية، بوزن (٢٥ ± ٠,٥) كجم وعمر (٢ ± ٠,٥) سنة. تم تقسيم الحيوانات التجريبية عشوائيًا إلى مجموعتين متساويتين. تحت التخدير العام، خضعت جميع الحيوانات التجربة لكسر مستعرض محدث في الجزء القاصي من عظم الكعبرة باستخدام منشار سلكي.

في المجموعة الأولى (مجموعة السيطرة) تم ترك الكسر المستعرض دون إضافة أي مادة، ثم تم إجراء الارجاع والتثبيت بشريط صب الألياف الزجاجية، في المجموعة الثانية (المجموعة المعالجة) تم المعالجة بوضع جسيمات السيلينيوم النانوية (Se-NPs) على خط الكسر، ثم تم إجراء الارجاع والتثبيت بشريط صب الألياف الزجاجية. تم تقييم تأثير جسيمات السيلينيوم النانوية على التئام الكسر من خلال المراقبة السريرية والفحص بالأشعة السينية والفحص النسيجي المرضي في الأسبوع الثاني والرابع والسادس والثامن من اجراء العمل الجراحي.

أظهر الفحص السريري للكلاب عودة أسرع إلى الحالة الطبيعية في المجموعة المعالجة مقارنة مع مجموعة السيطرة من خلال اختفاء العرج المبكر وتحمل الوزن المبكر على الطرف المصاب. أظهر الفحص بالأشعة السينية التئام الكسر بشكل أفضل في المجموعة المعالجة وأسرع من مجموعة السيطرة، وذلك من خلال زيادة التفاعل السمحاقي في بداية الالتئام، ثم بعد ذلك زيادة في تكوين الدشبذ وسرعة في اعادة تشكيل العظم أسرع مما في مجموع السيطرة. كما وأظهر الفحص المجهري تفوق المجموعة المعالجة من حيث الاستجابة الجيدة لالتئام الكسر، وذلك من خلال تكوين الانسجة الغضروفية الليفية حول منطقة الكسر في نهاية الدراسة عاد العظم الشكل والحجم شبه الطبيعي. حيث اظهر الفحص النسيجي المجهري تفوق مجموعة المعالجة في تكون الانسجة الغضروفية الليفية في بداية الالتئام، وزيادة في بانيات العظم وقلة في ناقضات العظم في الفترة الوسطية مع تكوين نظام هافرس مع التجمع المنتظم للخلايا العظمية حول قنوات هافرس، وفي المراحل النهائية ظهر العظم الصفائحي الكثيف، العظم الناضج الذي يحتوي على الخلايا العظمية داخل فجواته.

وكان استنتاج هذه الدراسة أن جسيمات السيلينيوم النانوية يمكن أن تسرع وتعزز التئام العظام في كسر الكعبرة القاصي.

تأثير جزيئات السيلينيوم النانوية على التئام كسر عظم الكعبرة المستحدث في الكلاب

رسالة ماجستير تقدم بها

مروان محمود عبد خلف

إلى

مجلس كلية الطب البيطري في جامعة الموصل
وهي جزء من متطلبات نيل شهادة الماجستير
في اختصاص الطب البيطري / الجراحة البيطرية

بإشراف
الاستاذ المساعد الدكتور
عمر عادل بدر

١٤٤٦ هـ ٢٠٢٥ م

جامعة الموصل
كلية الطب البيطري

تأثير جزيئات السيلينيوم النانوية على التئام كسر عظم الكعبرة المستحدث في الكلاب

مروان محمود عبد خلف

رسالة ماجستير

الطب البيطري / الجراحة البيطرية

بإشراف
الاستاذ المساعد الدكتور
عمر عادل بدر

١٤٤٦ هـ
٢٠٢٥ م